

Chapter 2

Modulation and Detection

Abstract In this chapter, we present a number of topics surrounding modulation and demodulation. We begin by introducing system-level block diagrams of AM and FM/PM modulators and demodulators, and explaining their respective principles of operation. In particular, under the topic of AM Modulator/Demodulator, we introduce the full carrier modulator, the single sideband suppressed carrier modulator, the double sideband suppressed carrier modulator, the envelope detector, and the synchronous detector. Under the topic of FM and PM Modulator/Demodulator, we introduce the VCO as FM modulator, the indirect FM modulator, the PM modulator, the balanced discriminator FM demodulator, the quadrature FM detector, the PLL-based FM detector, the zero-crossing FM detector, and the PM demodulator. Then, under the topic of digital modulation, we introduce the concepts of Nyquist Limit, data rate, Shannon Limit, information capacity, and bandwidth efficiency, as well as specific modulation schemes, such as, binary modulation, amplitude-shift keying (BASK), frequency-shift keying (BFSK), and phase-shift keying (BPSK), differential binary phase-shift keying (DBPSK), quadrature phase-shift keying (QPSK), $\pi/4$ shifted QPSK, minimum shift keying (MSK), M-ary quadrature amplitude modulation (QAM), orthogonal frequency division multiplexing (OFDM), direct sequence spread spectrum (DS/SS), and frequency hopping spread spectrum (FH/SS). We also introduce the geometric representation of digital modulation schemes and the complex envelope form of a modulation signal.

2.1 AM Modulators

An AM modulator, which implements the equation,

$$v_{AM}(t) = a_0 [1 + mg(t)] \cos \omega_0 t \quad (2.1)$$

may be represented as shown in Fig. 2.1. It is seen that the magnitude of the modulation index, m , if too large may cause distortion of the resulting modulated signal.

The corresponding frequency spectrum for the AM signal is given by [1],

$$F_M(\omega) = \frac{a_0}{2} [2\pi\delta(\omega - \omega_0) + 2\pi\delta(\omega + \omega_0) + F_B(\omega - \omega_0) + F_B(\omega + \omega_0)] \quad (2.2)$$

which is depicted in Fig. 2.2. As can be seen, due to symmetry with respect to the origin, the same information is carried in both the upper (centered at $+\omega_0$) and lower

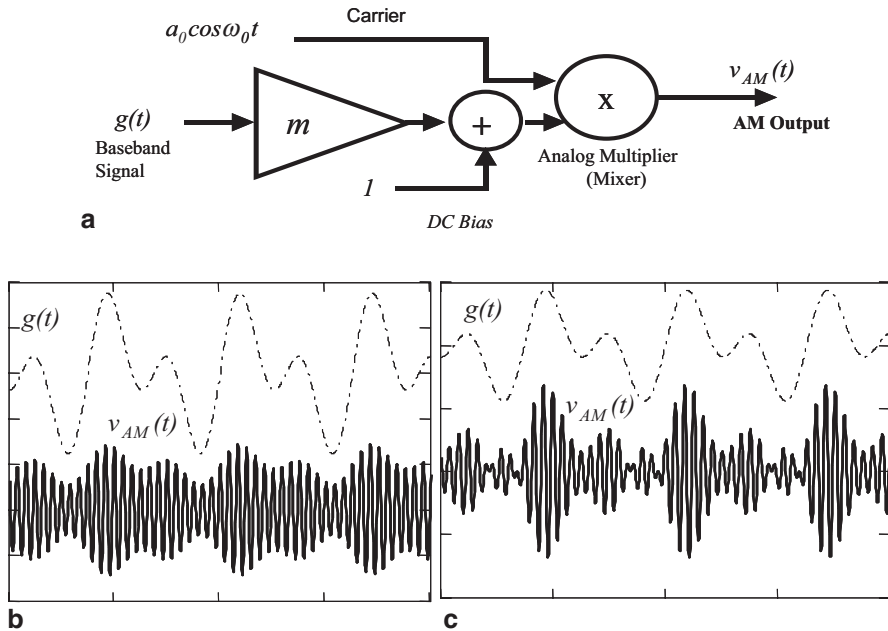


Fig. 2.1 **a** Depiction of system-level block diagram of AM modulator. **b** Depiction of modulating function, $g(t)$, and resulting modulated function, $v_{AM}(t)$ for the case of a correctly modulated AM signal, in which $(1 + mg(t)) > 0$. **c** Depiction of modulating function, $g(t)$, and resulting modulated function, $v_{AM}(t)$ for the case of an incorrectly modulated AM signal, in which $(1 + mg(t)) < 0$. In this case the modulation index, m , is too large and it causes distortions in the amplitude envelope. After [1]

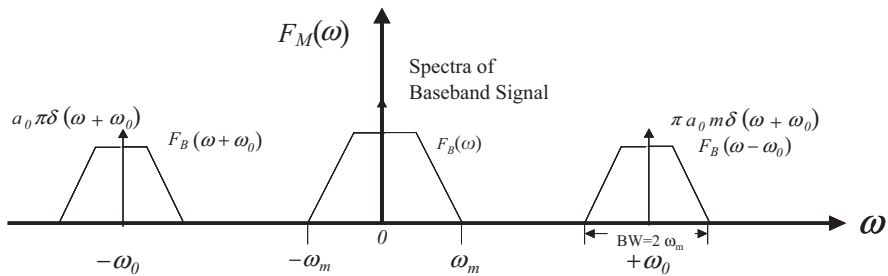


Fig. 2.2 Spectra of AM signal. The spectra of the baseband signal, centered at zero frequency, possess a maximum frequency ω_m

(centered at $-\omega_0$) sidebands. Therefore, not only one of them is redundant, but the transmitted power is split between the two sidebands. Finally, the modulated signal, centered on ω_0 , occupies twice ω_m , i.e.,

$$BW_{AM} = 2\omega_m \quad (2.3)$$

The excess, unnecessary, power and bandwidth accompanying the AM signal represented by (2.2), motivated another scheme to eliminate one of the sidebands, namely, *single sideband* AM or SSB modulation.

Fig. 2.3 Depiction of filtering method for producing a single sideband (SSB) AM signal. After [1]

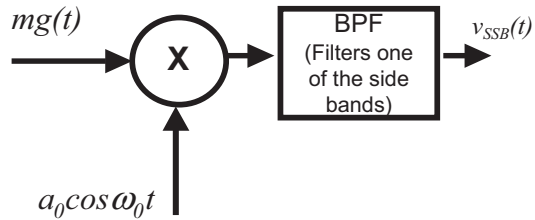
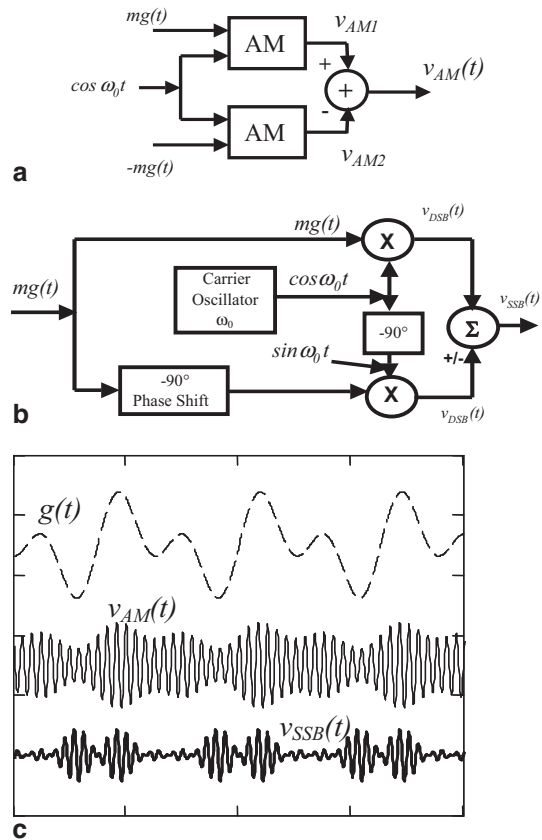


Fig. 2.4 a, b Block diagram depicting the balanced modulator method to create a single sideband AM signal. **c** Modulation signal, $g(t)$, resulting modulated signal with full carrier, $v_{AM}(t)$, and resulting modulated signal with suppressed carrier, $v_{SSB}(t)$. After [1]



2.1.1 Methods to Create Single Sideband (SSB) AM Signals

Two main methods to create an SSB signal are presented, namely, the filtering method and the balanced modulation method. In the filtering method, whose block diagram is presented in Fig. 2.3, one of the sidebands is eliminated by direct filtering.

In the balanced modulator method, the carrier is modulated with both $+g(t)$, and $-g(t)$, and then subtracted, as depicted in Fig. 2.4a. This operation is implemented by the block diagram shown in Fig. 2.4b (for the case in which there is no DC added to $g(t)$), and results in the waveforms $v_{SSB}(t)$ shown in Fig. 2.4c [1].

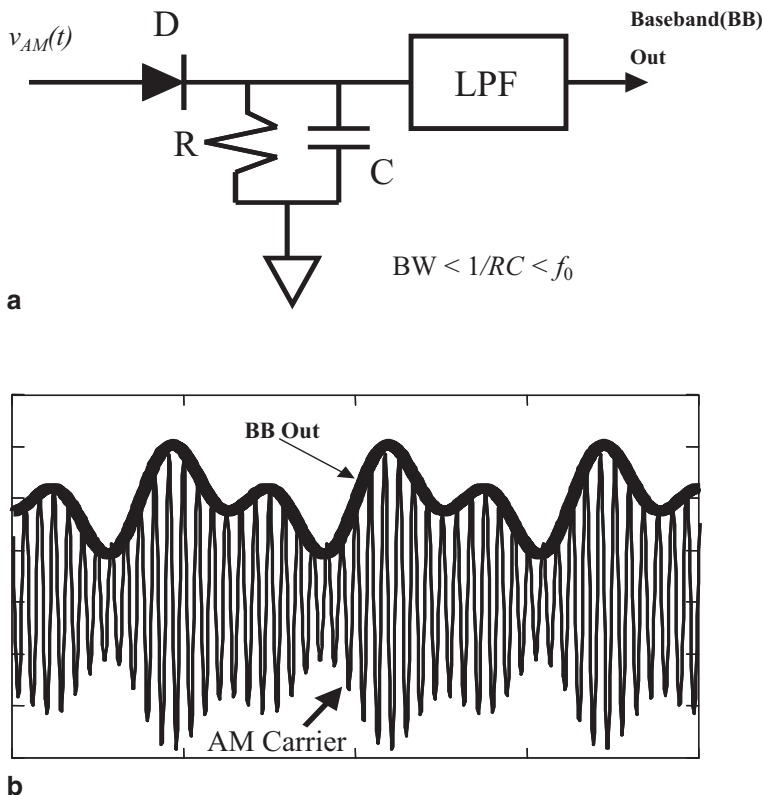


Fig. 2.5 **a** Envelope detector circuit plus lowpass filter. **b** Modulated AM signal, $v_{AM}(t)$. The high frequency carrier signal is filtered by the RC circuit. The modulating (baseband) *envelope* signal, $g(t)$, is extracted out of all its harmonics, by the lowpass filter and delivered to the output as BB. After [1]

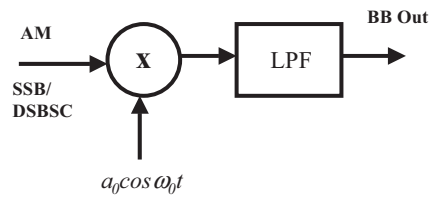
2.2 AM Demodulators

A variety of schemes are available to demodulate, i.e., to extract, the information-bearing signal, $g(t)$, from the received signal $v_{AM}(t)$ or $V_{SSB}(t)$; these are discussed next.

2.2.1 Envelope Detector

The *Envelope Detector* followed by a lowpass filter is perhaps the most fundamental AM demodulation system, Fig. 2.5. In this circuit, the received input signal is rectified by a diode, D , and passed by an RC filter which, with an inverse time constant greater than the modulating signal bandwidth, but smaller than the carrier frequency, is not responsive to the high-frequency carrier, but only to the modulating signal, the signal envelope and its harmonics. The harmonics are then attenuated, by a lowpass filter which selects the modulating signal [1].

Fig. 2.6 Product detector plus lowpass filter. When the locally generated carrier is synchronized to the transmitter, the circuit is called *synchronous detector*. After [1]



2.2.2 Product Detector

In the product detector, the incoming signal is multiplied by a locally generated carrier, and the resulting signal is passed through a lowpass filter, Fig. 2.6 [1]. In particular, the product of the incoming signal with the locally generated carrier yields,

$$\begin{aligned} K[1 + mg(t)]\cos^2 \omega_0 t &= K[1 + mg(t)] \cdot \frac{1}{2}(1 + \cos 2\omega_0 t) \\ &\rightarrow K[1 + mg(t)] \cdot \frac{1}{2} + K[1 + mg(t)] \cdot \frac{1}{2} \cdot \cos 2\omega_0 t \end{aligned} \quad (2.4)$$

which contains a first term whose spectral content is that of the baseband signal, and a second term whose spectrum is centered at twice the carrier frequency, i.e., the second term yields a double-sideband suppressed carrier (DSBC) signal. Therefore, at the output of the lowpass filter, only the baseband signal remains.

2.3 FM Modulators

Two FM demodulators will be presented, namely, the direct and the *indirect* methods.

2.3.1 Direct FM Modulator

The direct FM modulator uses a voltage controlled oscillator, Fig. 2.7.

In this circuit, the VCO has a free-running frequency, f_0 , given by,

$$f_0 = \frac{1}{2\pi\sqrt{L_0 C_0}} \quad (2.5)$$

This frequency is modulated by changing the value of frequency-determining capacitors (varactors) through the application of the baseband signal. In particular, the VCO output frequency becomes a time-dependent function given by,

$$f(t) = f_0 + kg(t) \quad (2.6)$$

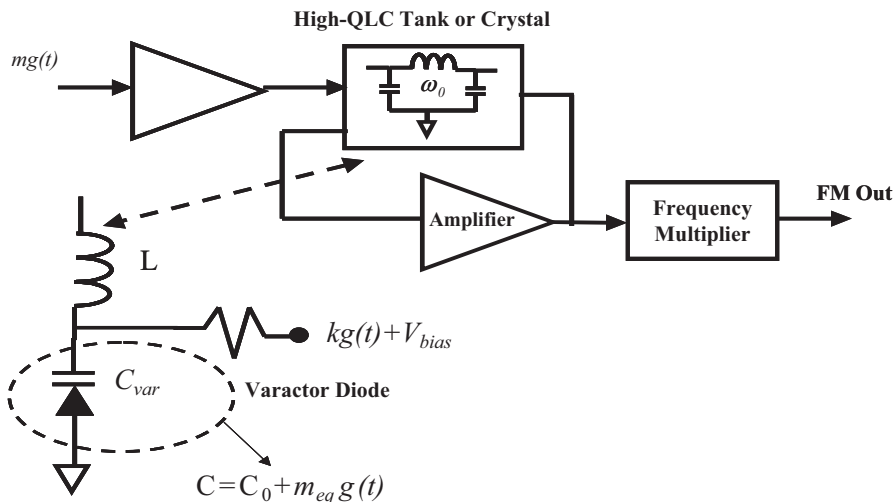
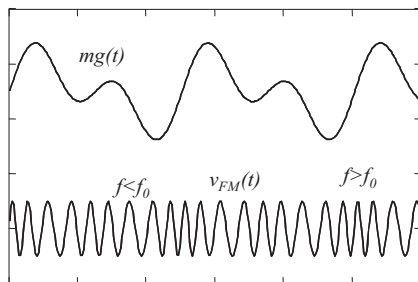


Fig. 2.7 Voltage-controlled oscillator (VCO) as FM modulator. After [1]

Fig. 2.8 Baseband signal (top) and frequency modulated carrier (bottom). After [1]



As the amplitude of the baseband signal increases and decreases, the carrier frequency follows, Fig. 2.8 [1].

2.3.2 Indirect FM Modulator

Rather than modulating the varactor voltage of a VCO, in the indirect FM method the modulating signal is first integrated, then used to phase-modulate a crystal-controlled carrier frequency. The signal is then multiplied for producing a wideband FM signal. The block diagram of an indirect FM modulator is shown in Fig. 2.9.

2.3.3 PM Modulator

To effect phase modulation, the constant carrier signal is generated independently, and then passed through an LC circuit whose capacitance is modulated by the

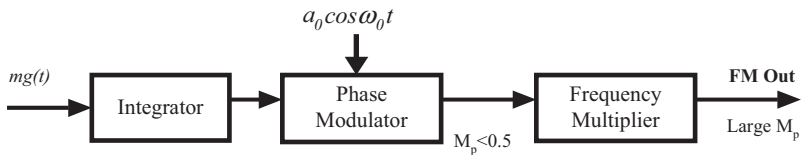
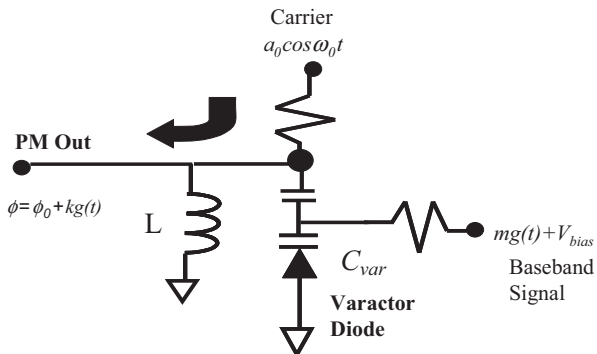


Fig. 2.9 Indirect FM modulator. *After* [1]

Fig. 2.10 Phase modulator circuit. *After* [1]



baseband signal, Fig. 2.10. For small varactor voltage swings, the LC circuit is linear and small phase shifts (a few degrees) are obtained. Larger deviations may be obtained using a frequency multiplier. The time-domain waveform of PM is similar to that of FM, and can only be distinguished from FM from knowledge of the source.

2.4 FM Demodulators

The various methods for effecting FM demodulation may be surmised from examining the FM waveform, namely [1],

$$v_{FM}(t) = A \cos \varphi(t) = A \cos \left[\omega_0 t + K \int g(t) dt \right] \quad (2.7)$$

In the first place, differentiating the instantaneous frequency,

$$\omega_i(t) = \frac{d\varphi(t)}{dt} = \omega_0 + K g(t) \quad (2.8)$$

it is seen that we get the desired output $g(t)$, if we cancel ω_0 .

On the other hand, differentiating $v_{FM}(t)$, we obtain:

$$\begin{aligned} \frac{dv_{FM}(t)}{dt} &= -A \sin \varphi(t) \frac{d\varphi}{dt} \\ &= -A [\omega_0 + K g(t)] \sin \varphi(t) \end{aligned} \quad (2.9)$$

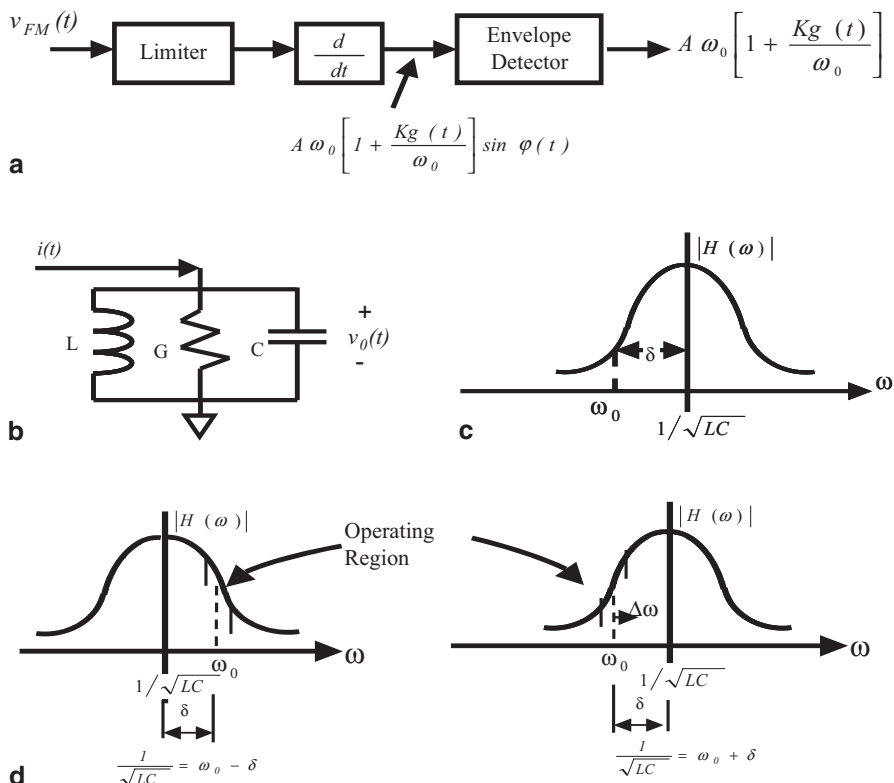


Fig. 2.11 **a** FM detector block diagram. **b** Circuit implementing differentiation (d/dt) block. **c** Transfer function of GLC circuit in **b**. **d** Relation of frequency deviation to operating region.

which looks like the an AM signal with envelope given by,

$$A[\omega_0 + Kg(t)] = A\omega_0 \left[1 + \frac{Kg(t)}{\omega_0} \right] \quad (2.10)$$

Therefore, we may obtain $g(t)$ by the envelope-detecting operation $dv_{FM}(t)/dt$.

2.4.1 FM Balanced Demodulator

The *balanced demodulator* implements FM demodulation as shown in Fig. 2.11a. In this block diagram, the *limiter* is inserted, prior to differentiation, to ensure that no terms coming from A result when the derivative is taken (otherwise these variations in A may obscure the true amplitude variations due to $g(t)$) [2].

Then, middle block in Fig. 2.11a, differentiation, $dv_{FM}(t)/dt$, is effected, which results in a signal whose amplitude is modulated by $g(t)$; this is like an AM signal with high-frequency carrier $\phi(t)$. The differentiation is implemented by a parallel GLC circuit, Fig. 2.11b, with transfer function,

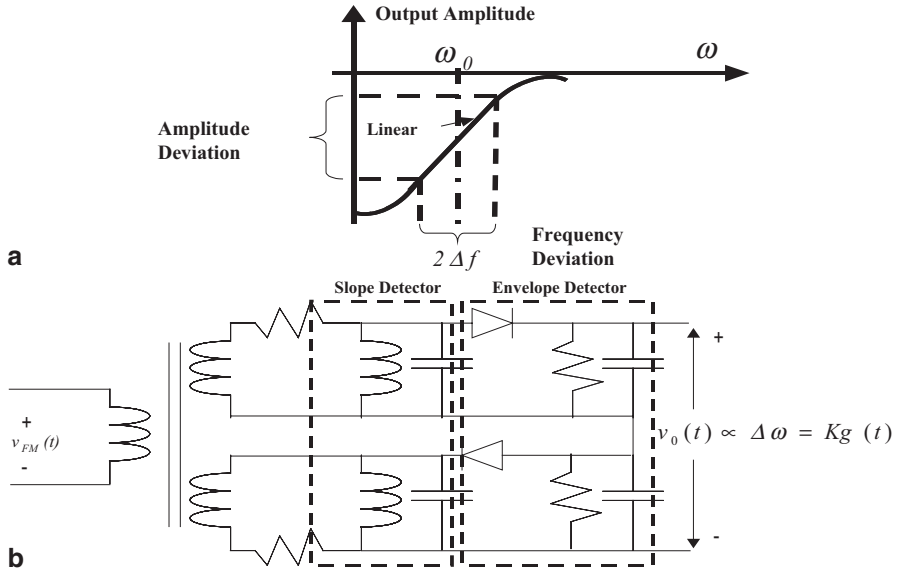


Fig. 2.12 **a** Characteristic of differentiation circuit, where a frequency deviation is translated into an amplitude deviation. **b** Balanced FM demodulator circuit differentiates and then detects FM signal, extracting baseband signal

$$|H(\omega)| = \left| \frac{V_0(\omega)}{I(\omega)} \right| = \frac{1/G}{\sqrt{1 + (\omega C - 1/\omega L)^2/G^2}} \quad (2.11)$$

The circuit has a damping $\alpha = G/2C$, and resonance frequency $1/\sqrt{LC}$, which is a distance δ from the carrier frequency, ω_0 . If the carrier frequency, ω_0 , is set at the middle of the positive slope of the transfer curve, Fig. 2.11d, then it will deviate a distance $\Delta\omega$, so that $\frac{1}{\sqrt{LC}} = \omega_0 + \delta$ on this operating region, and $\frac{1}{\sqrt{LC}} = \omega_0 - \delta$ on negative slope operating region. Then, assuming $\Delta\omega \ll \omega_0$, $\delta \ll \alpha$, and $\delta \ll \omega_0$, it can be shown [2] that the difference between H evaluated at these points is given by,

$$|H|_{\omega_0 + \delta} - |H|_{\omega_0 - \delta} = \frac{2\delta}{G\alpha^2} \Delta\omega \quad (2.12)$$

It will be recalled that, differentiation of a function of time with respect to time, in the time domain, is proportional to multiplication by frequency in the frequency domain, i.e., $d/dt \rightarrow j\omega$. Therefore, (2.12) is the frequency domain representation of differentiation [2].

Within a small deviation about the *high* carrier frequency ω_0 , the slope of the transfer curve, H , is linear, Fig. 2.12a. While this differentiated signal is now an

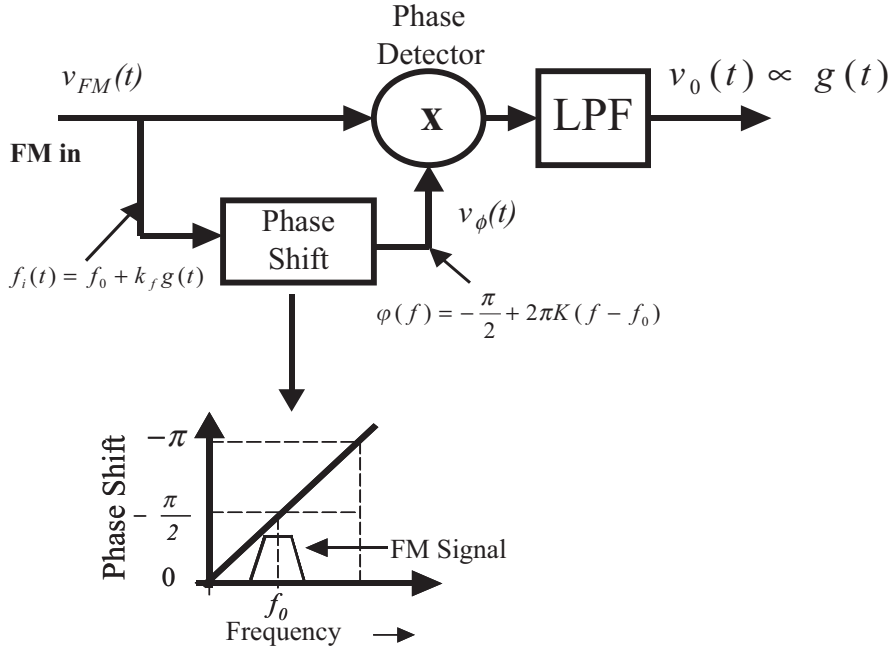


Fig. 2.13 FM demodulation by phase detector. After [1]

AM signal with its amplitude dictated by $g(t)$, but still at a high frequency, it must be passed by an envelope detector to remove the high-frequency carrier and finally extract $g(t)$. FM demodulation is, thus, completed by adding an envelope detector, Fig. 2.12b [1, 2], producing an output voltage given by,

$$v_0(t) \propto \Delta\omega = Kg(t) \quad (2.13)$$

2.4.2 FM Quadrature (Detector) Demodulator

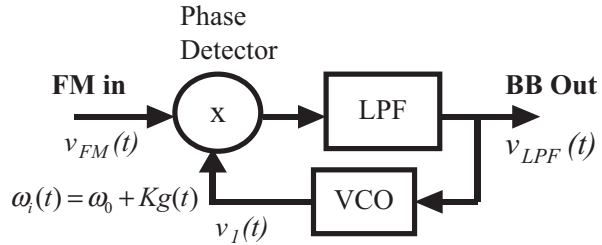
Examination of an FM signal reveals that its phase is shifted by an amount proportional to its instantaneous frequency (2.14).

$$v_{FM}(t) = A \cos(\omega_0 t + \phi(t)) \quad (2.14)$$

This fact is exploited by the product detector, Fig. 2.13 [1], to detect the phase difference between an incoming FM signal and the signal at the output of a phase shift network (2.15),

$$v_\phi(t) = A' \cos \left[2\pi f_0 t + 2\pi k_f \int g(t') dt' + \phi(f_i(t)) \right] \quad (2.15)$$

Fig. 2.14 Phase-locked loop as FM demodulator. *After* [1]



Since the phase shift introduced by the phase shift network is proportional to the instantaneous frequency of the input FM signal, the output voltage of the phase detector, after removing the high-frequency components by a lowpass filter, will also be proportional to the instantaneous frequency of the input FM signal, thus reproducing the original modulating signal, (2.16).

$$\begin{aligned} v_0(t) &= A'^2 \cos(\phi(f_i(t))) = A'^2 \cos\left(-\frac{\pi}{2} + 2\pi K(f_i(t) - f_0)\right) \\ &= A'^2 \sin[2\pi Kk_f g(t)] \propto g(t) \end{aligned} \quad (2.16)$$

The latter conclusions is clearly seen when one considers the series expansion of the sine function, which would contain the fundamental, which is proportional to $g(t)$, the third power of $g(t)$, etc. Thus, only the fundamental term, proportional to $g(t)$, would survive the lowpass filter, hence, (2.16).

2.4.3 Phase-Locked Loop (PLL)-Based FM Demodulator

The PLL, Fig. 2.14 [1], is a closed loop control system that tracks the variations in the received signal phase and frequency (2.17).

$$v_{FM}(t) = A \cos(\omega_0 + \Delta\omega)t \quad (2.17)$$

In this scheme, the VCO output,

$$v_1(t) = A_1 \cos(\omega_0 t + \varphi_1(t))t \quad (2.18)$$

where,

$$\omega_1 = \omega_0 + \frac{d\varphi_1(t)}{dt} \quad (2.19)$$

is compared with the input signal using a phase comparator (detector). The phase comparator produces an output voltage proportional to phase difference. The phase difference, in turn, is low-pass-filtered, producing $V_{LPF}(t)$, and fed back to the VCO to control its output frequency. The control of the VCO, $V_{LPF}(t)$, is itself the demodulated FM signal, $g(t)$ [1].

2.4.4 Zero-Crossing Detector FM Demodulator

As shown in the previous FM demodulation methods, they typically involve a frequency-to-amplitude (FM-to-AM) conversion. In the zero-crossing detector approach, the frequency-to-amplitude conversion operation is performed by counting the number of zero-crossings in the input FM signal; its principle of operation is as follows [3]. Given that the *instantaneous frequency deviation* in the FM signal is,

$$\omega_i = \omega_0 + \frac{d\varphi_i(t)}{dt} \quad (2.20)$$

then,

$$\int_{t_1}^{t_2} d\varphi(t) = \int_{t_1}^{t_2} 2\pi f_i(t) dt \quad (2.21)$$

from where, upon integration between adjacent zero-crossing times t_1 and t_2 , where $t_2 > t_1$, one obtains,

$$\varphi(t_2) - \varphi(t_1) = \int_{t_1}^{t_2} [2\pi f_0 + mg(t)] dt \quad (2.22)$$

But, also, because t_1 and t_2 are adjacent zero crossings, we must have,

$$\varphi(t_2) - \varphi(t_1) = \pi \quad (2.23)$$

or

$$[2\pi f_0 + mg(t)] \cdot (t_2 - t_1) \approx \pi \quad (2.24)$$

which, using $2\pi f_i(t)$, may be written as,

$$\pi \approx 2\pi f_i(t) \cdot (t_2 - t_1) \quad (2.25)$$

from where we obtain,

$$f_i(t) = \frac{1}{2\pi(t_2 - t_1)} \quad (2.26)$$

Now, since,

$$f_i(t) = f_0 + \frac{mg(t)}{2\pi} \quad (2.27)$$

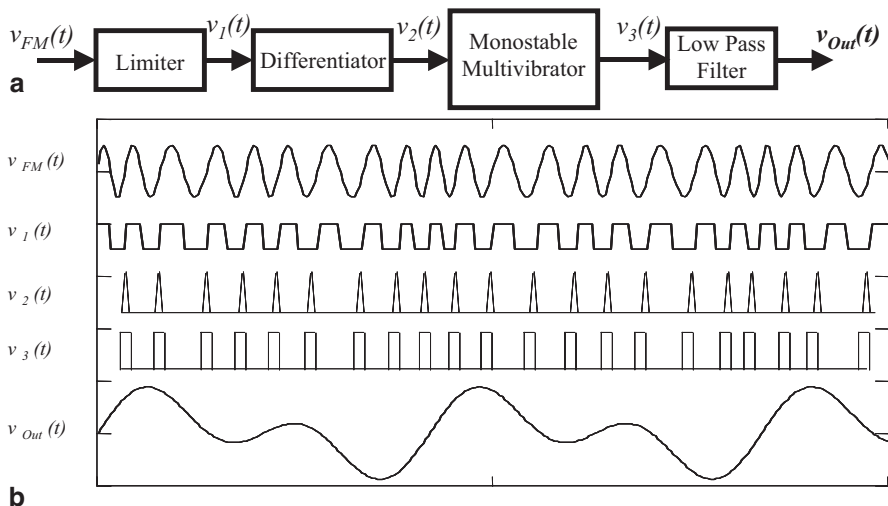
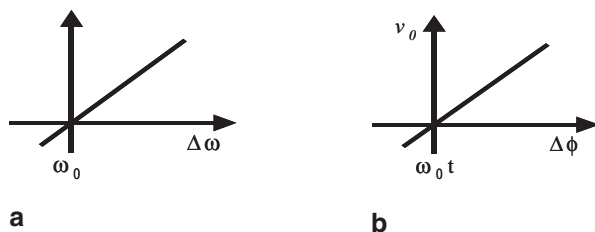


Fig. 2.15 **a** Block diagram of zero-crossing detector for FM demodulation. **b** Waveforms through-out the demodulator

Fig. 2.16 **a** FM demodulator transfer curve. **b** PM demodulator transfer curve



$g(t)$ may be found by measuring the spacing between zero-crossings in the interval $t_2 - t_1$.

The implementation of this method is depicted by the block diagram in Fig. 2.15 [3].

Following Fig. 2.15 (from top to bottom), the input FM signal, $v_{FM}(t)$, is applied to a limiter which, upon clipping the signal renders a rectangular pulse train, $v_1(t)$, reflecting the FM time variation. This FM pulse train, in turn, is applied to a differentiator, producing sharp pulses $v_2(t)$. These sharp pulses, coming out of the differentiator, are then employed as triggers to a monostable multivibrator (a “one shot”), which produces a pulse train $v_3(t)$, such that its average duration is proportional to the desired (modulating) baseband signal. Upon passing this pulse train by a lowpass filter, its average, a slowly varying DC component, $v_{Out}(t)$, is extracted; this is the desired demodulated signal, $g(t)$ [3].

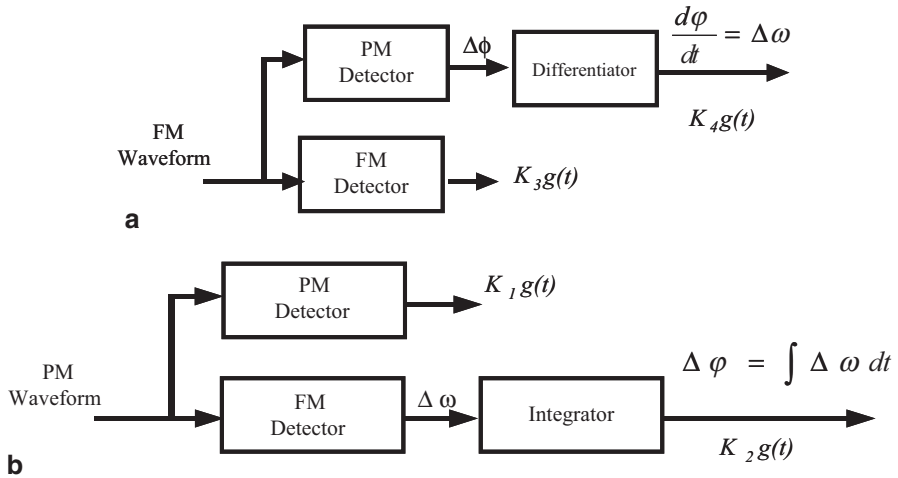


Fig. 2.17 a FM demodulator. b PM demodulator

2.5 PM Demodulators

As described in the last few sections, an FM demodulator consists of a circuit whose output voltage is proportional to the instantaneous *frequency* deviation, Fig. 2.16a. A PM demodulator, on the other hand, consists of a circuit whose output voltage is proportional to the instantaneous *phase* deviation, Fig. 2.16b [4].

Since the phase is the integral of the frequency, one should be able to perform the demodulation function for either type of demodulation, FM or PM, with a single detector, FM or PM, and an integrator or differentiator; this is shown in Fig. 2.17 [4].

2.6 Digital Modulation

In digital modulation, the carrier amplitude, frequency, or phase are made to vary (i.e., are modulated) according to a *digital representation* of the baseband signal. The first step in digital modulation, therefore, is to convert the baseband signal into a digital stream of bits. This entails sampling the baseband signal at a frequency f_s , and representing each sample by N quantization bits, Fig. 2.18 [1].

As is known, to enable recovery of the original signal from the sampled signal, the original signal must be sampled at a frequency greater than twice its maximum frequency, B_m . This is the so-called *Nyquist sampling rate limit*. If the original signal is sampled every $t_s = 1/f_s$ seconds, and every sample contains N bits, then the rate of creation of samples is $N/t_s = f_s N$ bits/s. This is the sampled data rate, R . It is said, then, that the original signal is represented by a *data rate* of R bits/s [1].

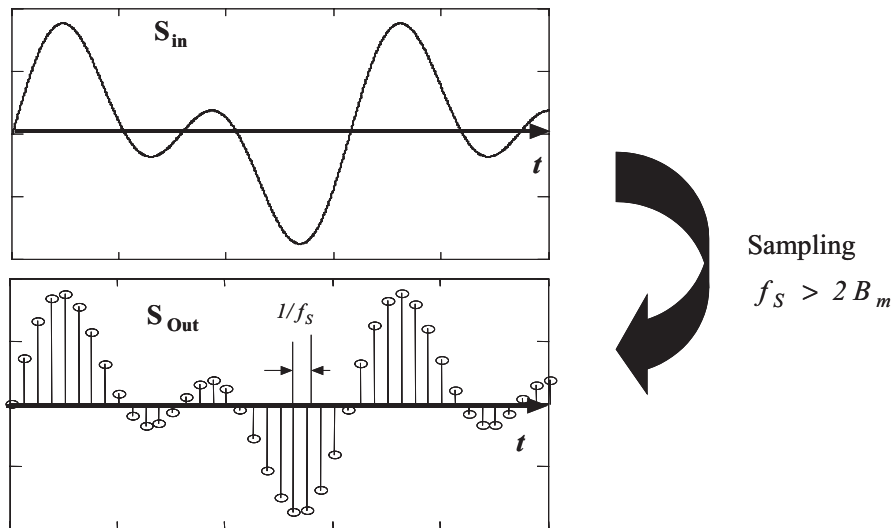


Fig. 2.18 Digitization of input baseband signal, S_{in} , via sampling at time intervals $1/f_s$, to produce a sampled output representation, S_{out} , where each sampling point is in turn represented by N bits. After [1]

The data rate, R , utilized in transmitting a given signal, may not be increased arbitrarily by increasing f_s , but it is limited by the bandwidth of the channel through which the signal travels. This capacity, in particular, is given by [1],

$$C = 2B \log_2 M \quad [\text{bits/sec}] \quad (2.28)$$

where B is the channel bandwidth and M is the number of bits utilized to represent a signal level being transmitted. For example, if we use two bits to represent a signal level, then $M=2$. If three bits, $M=3$, see Fig. 2.19. C is known as the *Shannon limit*, and represents the maximum bit rate allowed by a channel. It is evident from Fig. 2.19 that, while the resolution with which a given signal level may be represented increases with the number of bits utilized, the fact that the step-size decreases as M increases results in an increase in the likelihood that noise might "push" one level into the next, thus contributing to an error, i.e., it is easier for noise to confuse the true quantized level. A standardized parameter that may be used to compare channel capacity is the so-called *bandwidth efficiency*, which is given by [1],

$$\frac{C}{B} = 2 \log_2 M \quad [\text{bits/sec/Hz}] \quad (2.29)$$

A plot of bandwidth efficiency versus M is shown in Fig. 2.19.

A standardized parameter that may be used to compare channels is the so-called *bandwidth efficiency*, which is given by,

$$\frac{C}{B} = 2 \log_2 M \quad [\text{bits/sec/Hz}] \quad (2.30)$$

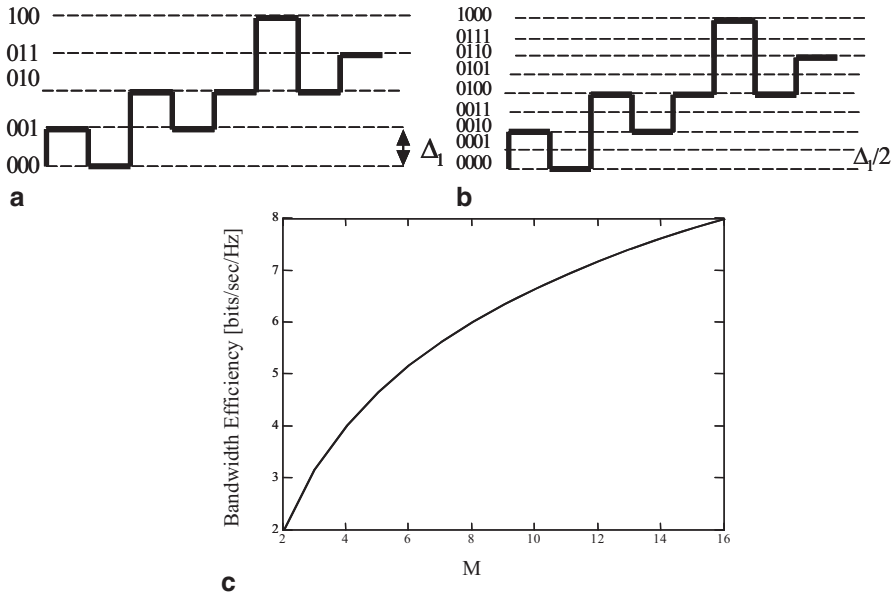


Fig. 2.19 Signal quantization. **a** Signal levels represented by 3 bits, i.e., $M=3$ bits. **b** Signal levels represented by 4 bits, i.e., $M=4$ bits. **c** Bandwidth efficiency versus number of bits representing a signal level. After [1]

A plot of bandwidth efficiency versus M is shown in Fig. For $M=3$, the maximum bandwidth efficiency would be 3.17.

A measure of channel capacity, that doesn't require that M be specified, is in terms of the signal-to-noise ratio (SNR). The SNR is defined as,

$$SNR = \frac{E_b R}{N_0 B} \quad (2.31)$$

where E_b is the average energy per bit, and N_0 is the noise power spectral density. In practice, $C < R$, therefore, one obtains,

$$\frac{C}{B} = \text{Log}_2 \left(1 + \frac{E_b}{N_0} \cdot \frac{R}{B} \right) \quad (2.32)$$

What this formula indicates is that, for a given noise level, N_0 , channel capacity is a function of the average energy per bit, E_b , expended [1–3].

2.6.1 Binary Modulation—Amplitude-Shift Keying (ASK)

When the baseband signal is quantized into two levels, $N=2$, it is represented by a binary stream of 1's and 0's. Binary modulation of the carrier amplitude is called

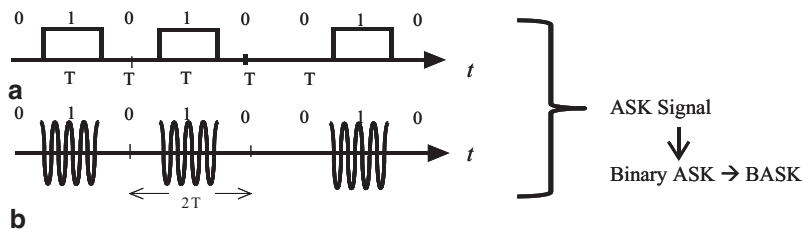


Fig. 2.20 Amplitude-Shift-Keying. **a** Binary signal. **b** Modulated signal. After [7]

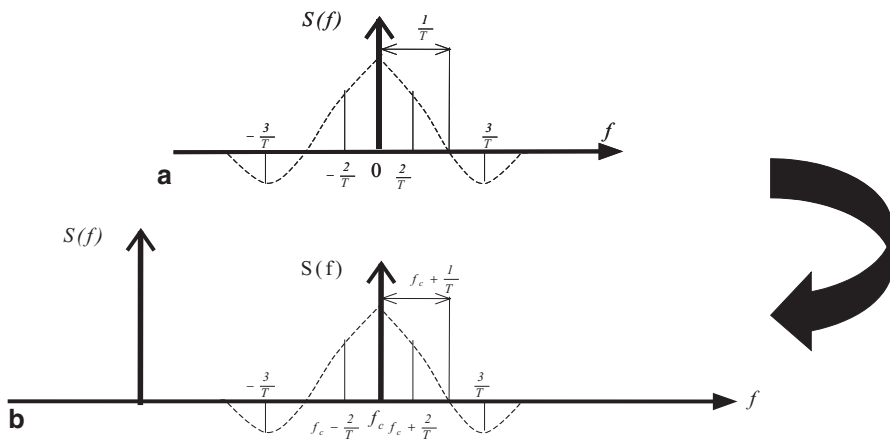


Fig. 2.21 **a** Spectrum of baseband signal. **b** Spectrum of ASK Wave (positive frequencies only). After [7]

ON-OFF Keying (OOK) or Amplitude-Shift-Keying (ASK), Fig. 2.20, whose corresponding spectrum is given in Fig. 2.21.

2.6.2 Binary Modulation—Frequency-Shift Keying (FSK)

Binary modulation of the carrier frequency is called Frequency-Shift Keying (FSK). In this scheme, as depicted in Fig. 2.22, the transmitted frequency is dictated by a binary sequence of 1's and 0's, according to which frequencies f_1 and f_0 are transmitted over intervals of time T ; the corresponding spectrum is as depicted in Fig. 2.23.

2.6.3 Binary Modulation—Phase-Shift Keying (PSK)

Binary modulation of the carrier phase is called Phase-Shift Keying (PSK). This is illustrated in Fig. 2.24. In this scheme, the phase of the carrier is shifted 180° in

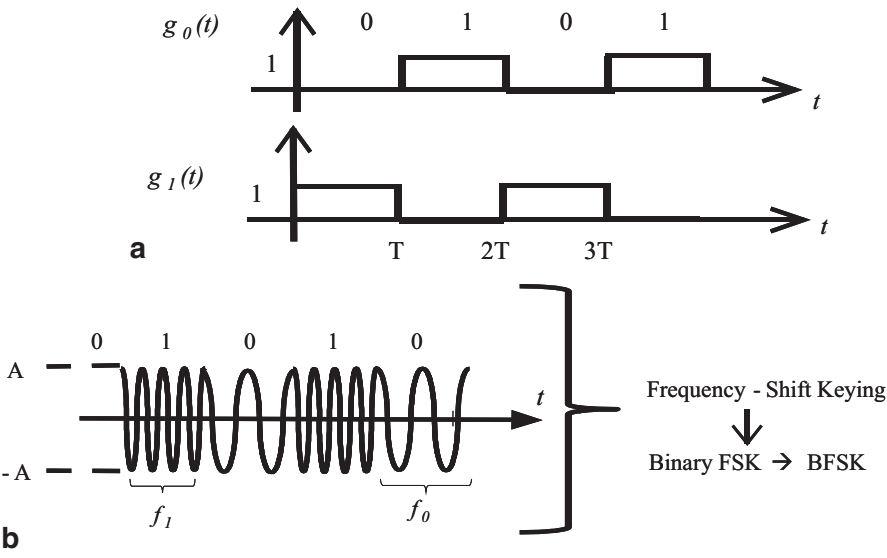


Fig. 2.22 Frequency-shift-keying. **a** Modulating binary signal. **b** FSK wave. *After [7]*

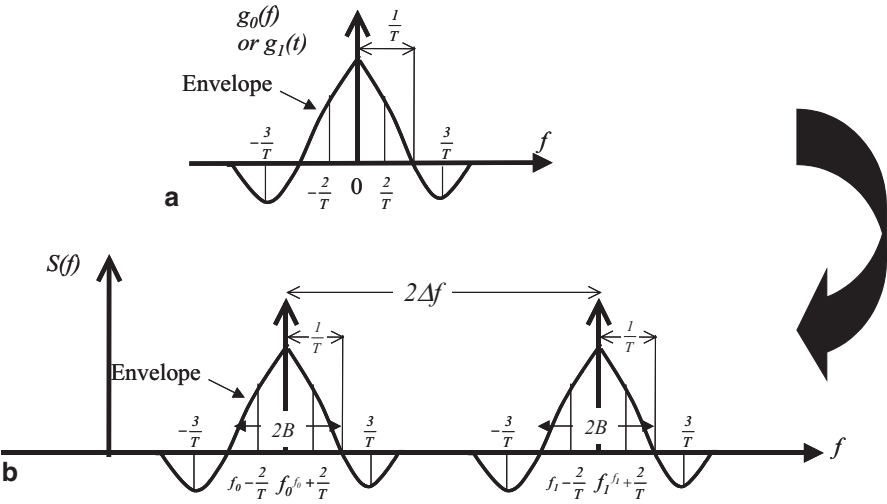


Fig. 2.23 **a** Spectrum of modulating baseband signal. **b** Spectrum of FSK Wave (positive frequencies only). *After [7]*

Fig. 2.24 **a** Modulating binary signal. **b** Phase-shift keying (Binary PSK \rightarrow BPSK). After [7]

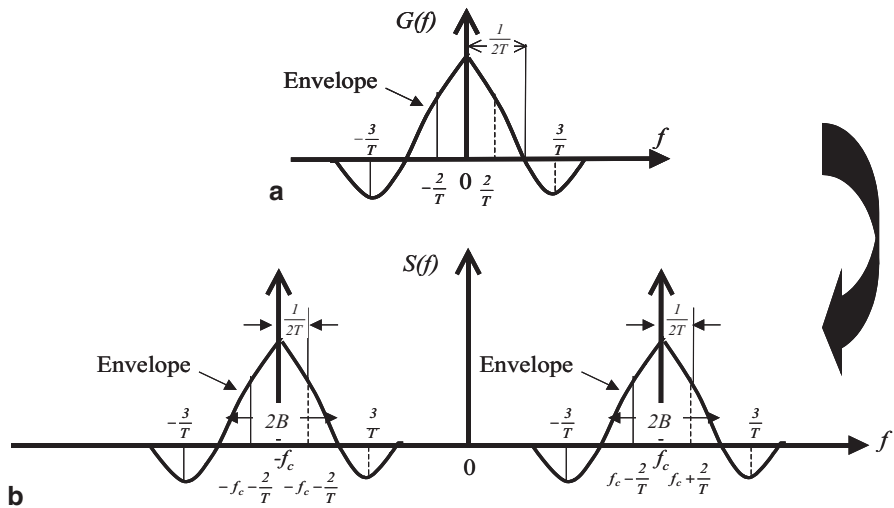
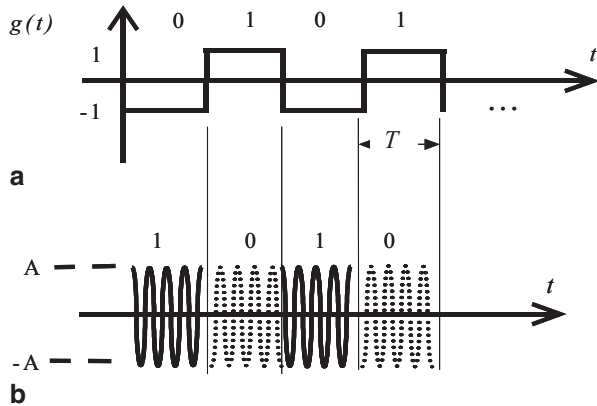


Fig. 2.25 **a** Spectrum of modulating baseband signal. **b** Spectrum of PSK wave. After [7]

accord with whether the modulating signal is a 1 or a 0. The pertinent spectrum is shown in Fig. 2.25.

2.7 Complex Envelope Form of Modulation Signals

Waveforms that are employed for digital modulation may be expressed in complex envelope form. [3, 5] i.e.

$$M(t) = I(t) + jQ(t) = A(t)e^{j\varphi(t)} \quad (2.33)$$

where $I(t)$ and $Q(t)$ represent in-phase and quadrature envelope waveforms, respectively, and have the following forms,

$$I(t) = \sum_k I_k p_I(t - kT_s - \tau) \quad (2.34)$$

$$Q(t) = \sum_k Q_k p_Q(t - kT_s - \tau) \quad (2.35)$$

where I_k and Q_k represent sequences of discrete variables mapped from the base-band (information) data with a symbol rate of $1/T_s$, $p_I(t)$ and $p_Q(t)$ represent finite energy pulses, such as rectangular or Gaussian, τ is a possible delay, and $A(t)$ and $\phi(t)$ are the envelope amplitude and phase, respectively [3, 5]. The amplitude and phase in (2.33) are given by,

$$A(t) = \sqrt{I^2(t) + Q^2(t)} \quad (2.36)$$

$$\phi(t) = \tan^{-1} \frac{Q(t)}{I(t)} \quad (2.37)$$

The symbol duration, T_s , of an M -ary keying modulation is related to the bit duration T_b of the originally binary data stream as,

$$T_s = \log_2 M \cdot T_b \quad (2.38)$$

Digital modulation beyond binary (i.e., with more than two levels) usually exploits the I and Q representation.

2.7.1 M -ary Modulation—MPSK

The representation of these modulation schemes is better visualized via the concept of constellations. We begin this subject by introducing the *geometric* representation of modulation signals.

If there are M possible signals, the modulation signal set S can be represented as [5]:

$$S = \{s_1(t), s_2(t), \dots, s_M(t)\} \quad (2.39)$$

While for binary modulation schemes, a binary information bit is mapped directly to a signal and S will contain only two signals, for higher-level modulation schemes (M -ary keying) the signal set will contain more than two signals; each signal (or *symbol*) will represent more than a single bit of information.

With a signal set of size M , it is possible to transmit a maximum of $\log_2 M$ bits of information per symbol. Since the elements of S may be viewed as points in a vector space, the representations are called *constellations*. When the baseband signal is

quantized into M levels, $N=M$, it is represented by an M -ary stream of 1's and 0's. Now, from the fact that any finite set of physically realizable waveforms in a vector space can be expressed as a linear combination of N orthonormal waveforms, which form the basis of that vector space, representing the modulation signals on a vector space, requires finding a set of signals that form a basis for that vector space. Once a basis is determined, any point in that vector space can be represented as a linear combination of the basis signals [3, 5],

$$\{\varphi_j(t) | j = 1, 2, \dots, N\} \quad (2.40)$$

such that,

$$s_i(t) = \sum_{j=1}^N s_{ij} \phi_j(t) \quad (2.41)$$

The basis signals are orthogonal to one another such that,

$$\int_{-\infty}^{\infty} \phi_i(t) \phi_j(t) dt = 0 \quad i \neq j \quad (2.42)$$

and each of the basis signals is normalized to have unit energy, i.e.,

$$E = \int_{-\infty}^{\infty} \phi_i^2(t) dt = 1 \quad (2.43)$$

2.7.2 Binary Phase Shift Keying Modulation—BPSK

In this digital modulation scheme, the phase of a constant envelope carrier is switched between two signals m_1 (bit 1) and m_2 (bit 0), the two phases being separated by 180° . The BPSK signal is [3],

$$s_{BPSK}(t) = \sqrt{\frac{2E_b}{T_b}} \cos(2\pi f_c t + \theta_c) \quad 0 \leq t \leq T_b \quad (\text{binary } 1) \quad (2.44)$$

or

$$s_{BPSK}(t) = -\sqrt{\frac{2E_b}{T_b}} \cos(2\pi f_c t + \theta_c) \quad 0 \leq t \leq T_b \quad (\text{binary } 0) \quad (2.45)$$

which may be written as,

$$s_{BPSK}(t) = m(t) \sqrt{\frac{2E_b}{T_b}} \cos(2\pi f_c t + \theta_c) \quad (2.46)$$

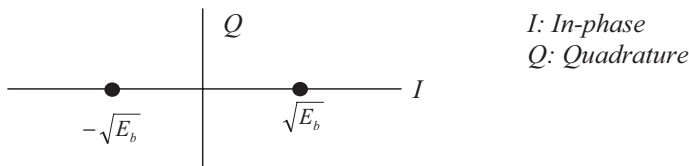


Fig. 2.26 BPSK constellation diagram

This is equivalent to double sideband suppressed carrier modulated waveform, where $m(t)$ is the modulating signal and $\cos(2\pi f_c t)$ is the carrier; it can be generated using a balance modulator.

Assuming a rectangular pulse ($p(t) = \text{rect}((t - T_b/2)T_b)$), for BPSK signals $s_1(t)$ and $s_2(t)$ given by,

$$s_1(t) = \sqrt{\frac{2E_b}{T_b}} \cos(2\pi f_c t) \quad 0 \leq t \leq T_b \quad (2.47)$$

and

$$s_2(t) = -\sqrt{\frac{2E_b}{T_b}} \cos(2\pi f_c t) \quad 0 \leq t \leq T_b \quad (2.48)$$

E_b and T_b are the energy and period per bit, respectively, $\phi_1(t)$ consists of a single waveform, namely,

$$\phi_1(t) = \sqrt{\frac{2}{T_b}} \cos(2\pi f_c t) \quad 0 \leq t \leq T_b \quad (2.49)$$

Using this basis signal, the BPSK signal set can be represented as,

$$S_{BPSK} = \{\sqrt{E_b} \phi_1(t), -\sqrt{E_b} \phi_1(t)\} \quad (2.50)$$

This signal set can be shown geometrically as in Fig. 2.26. This, so-called *constellation diagram*, provides a graphical representation of the complex envelope of each possible *symbol state*.

It should be noticed that [3, 5]: (1) The number of basis signals will always be less than or equal to the number of signals in the set. (In BPSK we have one basis signal, but two signals in the set); (2) The number of basis signals required to represent the complex modulation signal set is called the *dimension* of the vector space; (3) If there are as many basis signals as there are signals in the modulation signal set, then all the signals in the set are orthogonal to one another.

The properties of a modulation scheme that can be inferred from its constellation are as follows: (1) The bandwidth occupied by the modulation signals decreases as

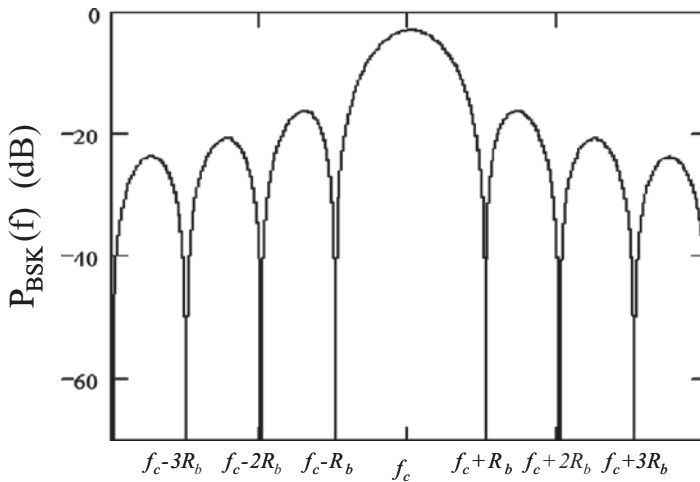


Fig. 2.27 Power spectral density for BPSK. The bandwidth, $BW = 2R_b = 2/T_b$

the number of signals/dimension increases, in particular, the more densely packed a constellation, the more bandwidth-efficient it is; (2) The bandwidth occupied by a modulated signal *increases* with the dimension N of the constellation; (3) The probability of bit error is proportional to the distance between the closest points in the constellation [3, 5].

It can be shown, that the typical power spectral density for BPSK is given by [3],

$$P_{BPSK}(f) = \frac{E_b}{2} \left[\left(\frac{\sin \pi(f - f_c)T_b}{\pi(f - f_c)T_b} \right)^2 + \left(\frac{\sin \pi(-f - f_c)T_b}{\pi(-f - f_c)T_b} \right)^2 \right] \quad (2.51)$$

This is plotted in Fig. 2.27. Further, the bandwidth containing the signal energy is a function of the shape of the pulse [3]. For a rectangular pulse, 90 % of signal energy is contained within a bandwidth $BW \sim 1.6R_b$, whereas for a raised cosine filtering pulse with $\alpha=0.5$, 100 % of signal is contained within a $BW = 1.5R_b$ [3].

2.7.2.1 Binary Phase Shift Keying Detection

The detection of a BPSK employs a *coherent* or *synchronous* demodulation approach to extract the modulated signal, Fig. 2.28. Accordingly, information about the carrier phase and frequency must be available at the receiver [5].

In particular, the received signal is first squared to generate a DC signal and a varying sinusoid at twice carrier frequency. The DC is filtered out and a frequency divider recreates the carrier which, multiplied by itself and lowpass-filtered results in the modulation signal $m(t)$ [3].

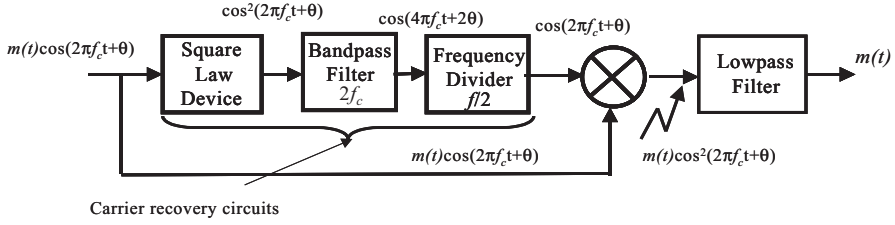


Fig. 2.28 BPSK demodulation circuit

$\{m_k\}$		1	0	0	1	0	1	1	0
$\{d_{k-1}\}$	1	1	0	0	1	1	0	0	0
$\{d_k\}$	1	1	0	1	1	0	0	0	1

$$d_k = \overline{m_k \oplus d_{k-1}}$$

Fig. 2.29 Illustration of differential BPSK. d_k is unchanged from previous symbol if $m_k = 1$, and d_k is toggled if $m_k = 0$

Assuming an additive white Gaussian noise channel (AWGN) with noise spectral density N_0 , the average probability of bit error for BPSK is a function of the energy per bit, E_b is given by [3],

$$P_{e,BPSK} = Q\left(\sqrt{\frac{2E_b}{N_0}}\right) \quad (2.52)$$

where,

$$Q(x) = \int_x^{\infty} \frac{1}{\sqrt{2\pi}} \exp(-x^2/2) dx \quad (2.53)$$

2.7.3 Differential Binary Phase Shift Keying—DBPSK

In the DBPSK modulation approach, the BPSK technique is employed in a *non-coherent* fashion to circumvent the need for a coherent reference signal at the receiver. In this scheme, the input binary sequence is first differentially encoded and then modulated using a BPSK modulator. In particular, the input binary sequence $\{m_k\}$ is used to generate a differentially encoded sequence $\{d_k\}$ by complementing the modulo-2 sum of m_k and d_{k-1} . Figure 2.29 illustrates the differential encoding process [3].

2.7.3.1 DPSK Modulator

To implement DBPSK modulation, a one-bit delay element and logic circuit generate a differentially encoded sequence, and then the differentially-encoded bit stream

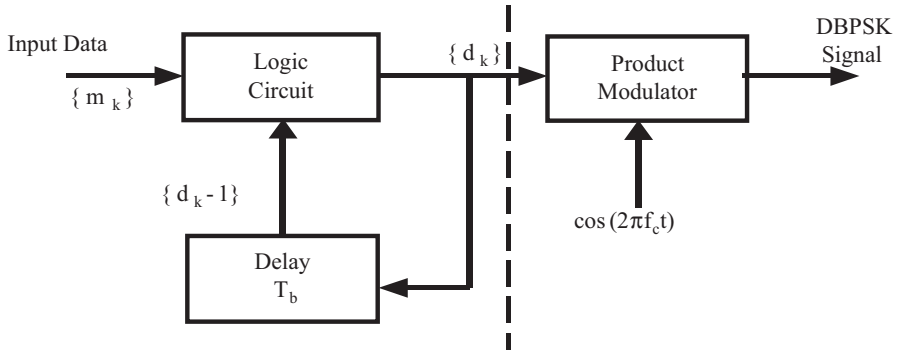


Fig. 2.30 DBPSK modulator

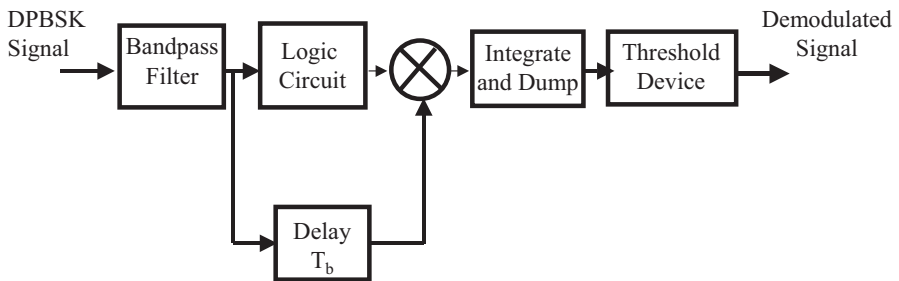


Fig. 2.31 DBPSK demodulator

is passed through a product modulator. This is depicted in the block diagram of Fig. 2.30 [3].

2.7.3.2 DPSK Demodulator

Implementation of the DPSK demodulator involves recovering the received sequence recovered through a process complementary to the modulation process, see Fig. 2.31 [3]. The approach exhibits a reduced receiver complexity, but at the expense of a 3dB inferior energy efficiency. The probability of bit errors is given by [3], [5],

$$P_{e,DPBSK} = \frac{1}{2} \exp\left(-\frac{E_b}{N_0}\right) \quad (2.54)$$

2.7.4 Quadrature Phase Shift Keying Modulation—QPSK

In this modulation scheme, the phase of the carrier takes on four equally-spaced values, namely, 0 , $\pi/2$, π , and $3\pi/2$, where each value of phase corresponds to a unique pair of baseband (message) bits given by [3, 5],

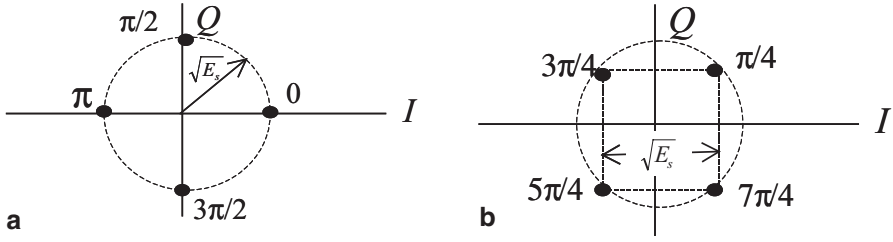


Fig. 2.32 QPSK Constellations

$$s_{QPSK}(t) = \sqrt{\frac{2E_b}{T_b}} \cos(2\pi f_c t + (i-1)\frac{\pi}{2}) \quad 0 \leq t \leq T_s \quad i = 1, 2, 3, 4 \quad (2.55)$$

$$s_{QPSK}(t) = \sqrt{\frac{2E_b}{T_b}} \cos\left[(i-1)\frac{\pi}{2}\right] \cos(2\pi f_c t) - \sqrt{\frac{2E_b}{T_b}} \sin\left[(i-1)\frac{\pi}{2}\right] \sin(2\pi f_c t) \quad (2.56)$$

With the basis functions:

$$\varphi_1(t) = \sqrt{\frac{2}{T_s}} \cos(2\pi f_c t) \quad (2.57)$$

and

$$\varphi_2(t) = \sqrt{\frac{2}{T_s}} \sin(2\pi f_c t) \quad (2.58)$$

the QPSK set is,

$$S_{QPSK} = \left\{ \sqrt{E_s} \cos\left[(i-1)\frac{\pi}{2}\right] \varphi_1(t), -\sqrt{E_s} \sin\left[(i-1)\frac{\pi}{2}\right] \varphi_2(t) \right\} \quad i = 1, 2, 3, 4 \quad (2.59)$$

and its geometrical constellation is as shown in Fig. 2.32. The constellations are equivalent; they differ by a 45-degree rotation.

It can be shown that the power spectral density for QPSK, see Fig. 2.33, is given by [3],

$$P_{QPSK}(f) = E_b \left[\left(\frac{\sin 2\pi(f - f_c)T_b}{\pi(f - f_c)T_b} \right)^2 + \left(\frac{\sin 2\pi(-f - f_c)T_b}{\pi(-f - f_c)T_b} \right)^2 \right] \quad (2.60)$$

The null-to-null BW = R_b , which is half of that of a BPSK signal [3, 5].

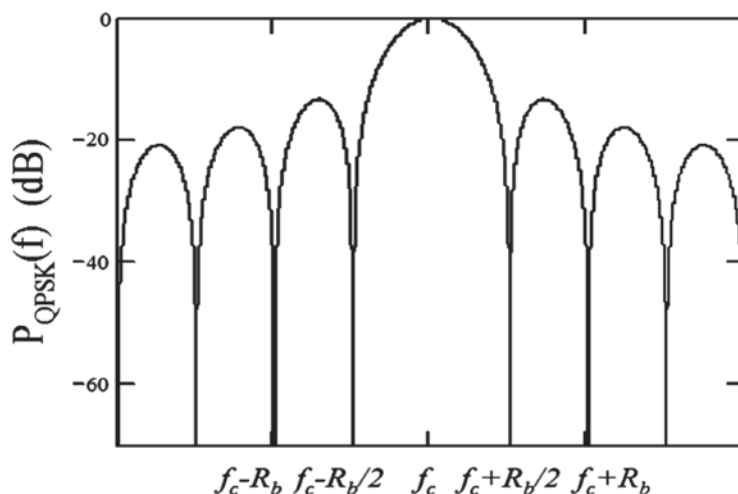


Fig. 2.33 Power spectral density for QPSK. The bandwidth, $BW = R_b$

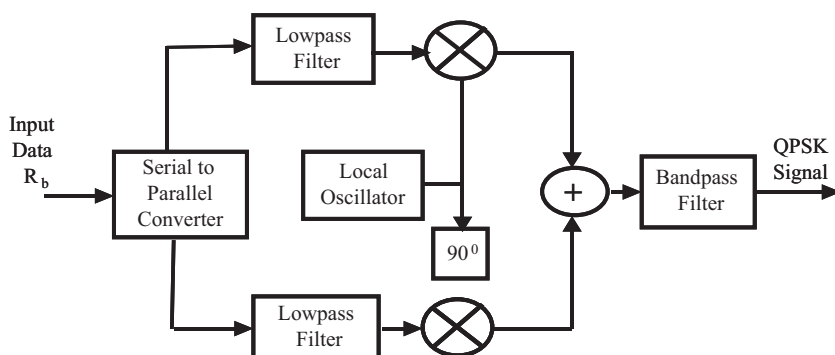


Fig. 2.34 QPSK modulator

2.7.4.1 Quadrature Phase Shift Keying Modulator

In the QPSK modulator, a unipolar bit stream $m(t)$ carrying the information signal at the rate R_b is first converted into a bipolar non-return-to-zero (NRZ) sequence. This sequence is then split into in-phase and quadrature components, $mI(t)$ and $mQ(t)$, each having a bit rate $R_b/2$. These two binary sequences, in turn, are separately modulated by two carriers, so that each is considered BPSK, and summed to produce the QPSK signal. In order to confine the power spectrum of the QPSK signal to its designated band, it is subsequently passed through a bandpass filter (BPF). A block diagram implementing the modulator is shown in Fig. 2.34 [3, 5].

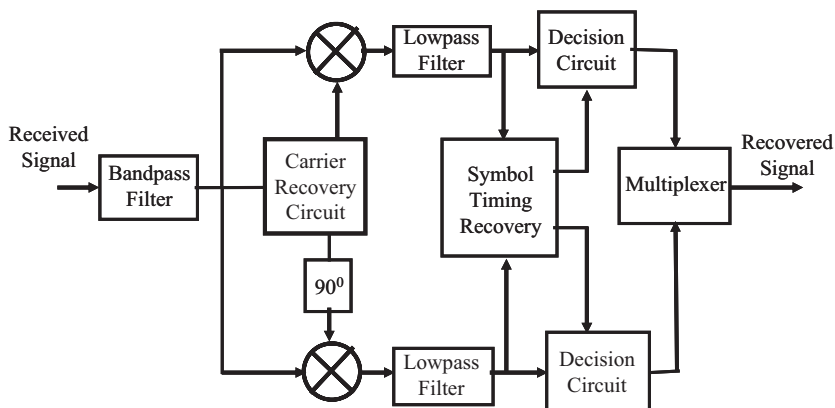
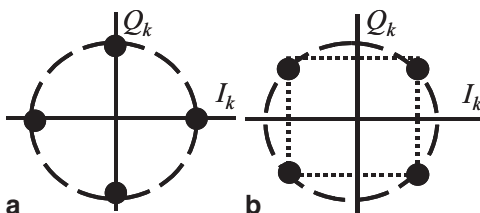


Fig. 2.35 QPSK demodulator

Fig. 2.36 $\pi/4$ QPSK constellations: **a** Possible states when $\theta_{k-1} = n\pi/2$. **b** Possible states when $\theta_{k-1} = n\pi/4$



2.7.4.2 Quadrature Phase Shift Keying Demodulator

The demodulator system for a QPSK-modulated signal is depicted by the block diagram in Fig. 2.35. The incoming QPSK signal is first filtered by a front-end bandpass filter to remove the out-of-band noise and adjacent channel interference accompanying it. Subsequently, the filtered output is split into two parts, each of which is then coherently demodulated using I and Q carriers. The coherent carriers used are recovered from the received signal using carrier recovery circuits as before (see BPSK). Next, the outputs of the demodulators are passed through decision circuits which generate I and Q streams. Finally, the two stream components are multiplexed to reproduce the original binary sequence [3, 5].

2.7.5 $\pi/4$ QPSK—Shifted Quadrature Phase-Shift Keying Modulation

In this scheme, two QPSK constellations, shifted by $\pi/4$ with respect to each other, are sampled to constitute the modulated signal. Selecting every successive bit by alternating between the two constellations, ensures that there is at least a shift which is an integer of $\pi/4$ radians between successive symbols. This guarantees that there

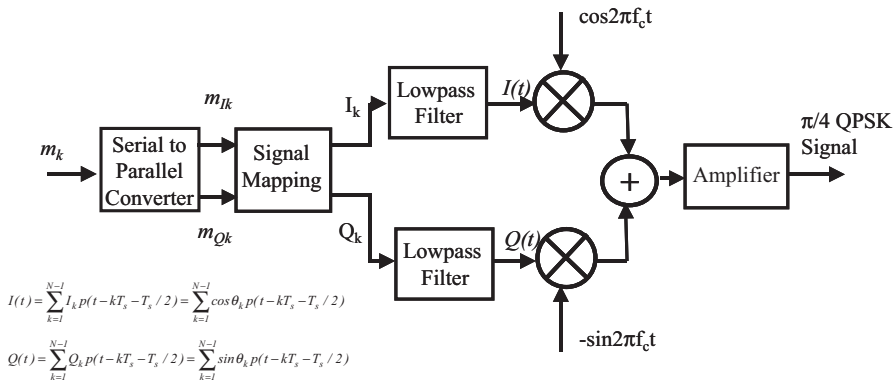


Fig. 2.37 $\pi/4$ QPSK modulator. Definition of variables: $I_k = \cos \theta_k = I_{k-1} \cos \phi_k - Q_{k-1} \sin \phi_k$; $Q_k \sin \theta_k = I_{k-1} \sin \phi_k + Q_{k-1} \cos \phi_k$; Phases of k th and $k-1$ st symbols $\theta_k = \theta_{k-1} + \phi_k$

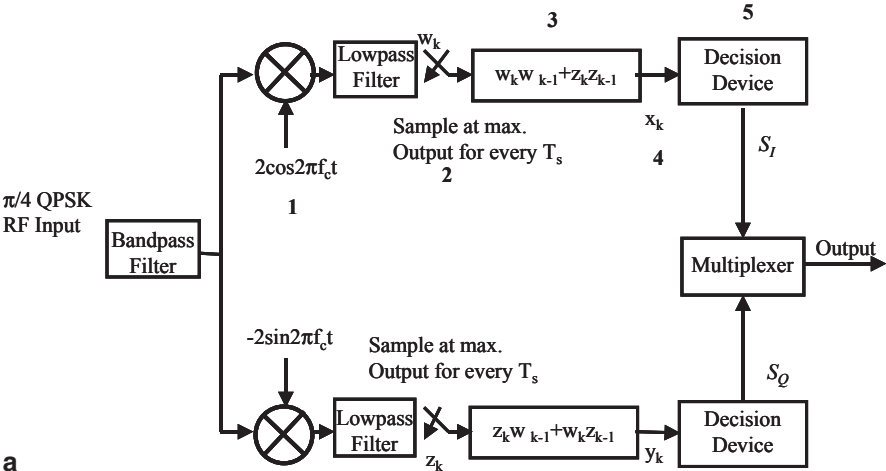
is a phase transition for every symbol, which enables a receiver to perform timing recovery and synchronization [3, 5]. Figure 2.36 depicts the two constellations.

2.7.5.1 $\pi/4$ QPSK—Shifted Quadrature Phase-Shift Keying Modulator

In the circuit implementation of this modulation scheme, Fig. 2.37, the input bit stream is first partitioned, by a serial-to-parallel converter, into $m_{I,k}$ and $m_{Q,k}$ parallel bit streams, where each symbol has a rate equal to half that of the incoming bit rate. Subsequently, each of the streams is applied to a signal mapping circuit which generates the k -th in-phase and quadrature pulses, I_k and Q_k , over the $kT < t < (k+1)T$ time interval. This is followed by the separate modulation of I_k and Q_k by two carriers which are then added to produce the $\pi/4$ QPSK signal [3]. The block diagram implementing this is shown in Fig. 2.37.

2.7.5.2 $\pi/4$ QPSK—Shifted Quadrature Phase-Shift Keying Demodulator

Demodulation of a $\pi/4$ QPSK signal proceeds as follows (the numbers correspond to those in diagram of Fig. 2.38): (1) The incoming $\pi/4$ QPSK signal is first quadrature-demodulated using two LO signals with the frequency identical to the transmitted carrier; (2) The output product is applied to lowpass filters, whose output is sampled at the maximum amplitude every T_s seconds; (3) The two sequences are then passed through differential decoders; (4) The output of differential decoder may be expressed as $x_k = \cos(\phi_k - \phi_{k-1})$, $y_k = \sin(\phi_k - \phi_{k-1})$; (5) The output of the differential decoder is applied to the decision circuit, which uses the table in Fig. 2.36(b) to determine the output bit as follows: $S_I = 1$, if $x_k > 0$ or $S_I = 0$, if $x_k < 0$ $S_Q = 1$, if $y_k > 0$ or $S_Q = 0$ if $y_k < 0$.



Information bits mI_k, mQ_k	Phase Shift ϕ_k
11	$\pi/4$
01	$3\pi/4$
00	$-3\pi/4$
10	$-\pi/4$

b

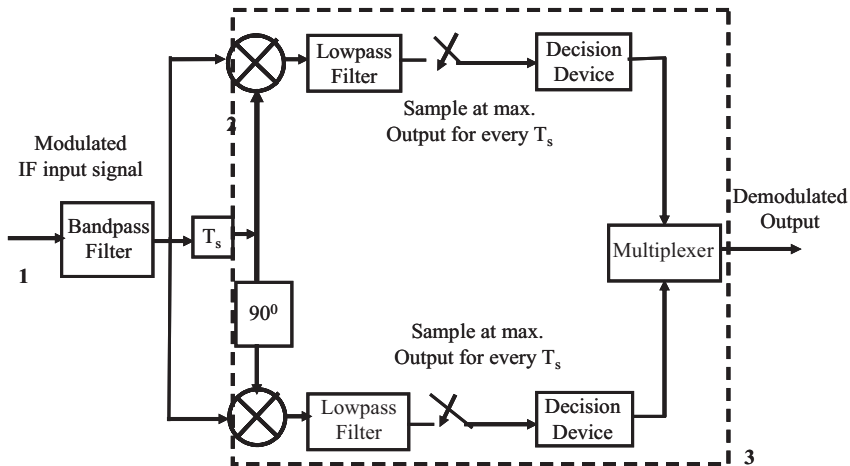
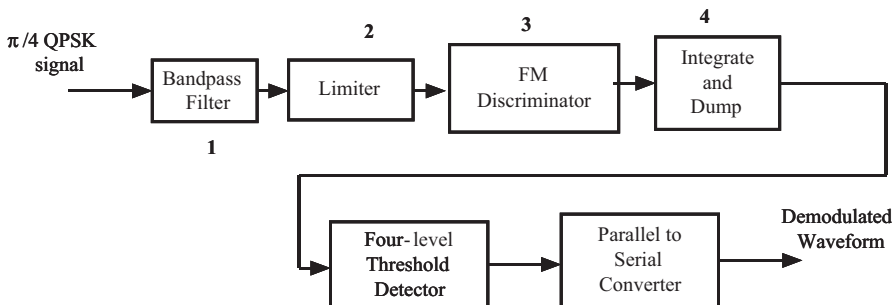
Fig. 2.38 **a** $\pi/4$ QPSK demodulator. Definition of variables: In-Phase: $w_k = \cos(\phi_k - \gamma)$; In Quadrature: $z_k = \sin(\phi_k - \gamma)$; $\phi_k = \tan^{-1}(Q_k / I_k)$; γ due to noise. **b** Carrier phase shift corresponding to various input bit pairs

2.7.5.3 $\pi/4$ Shifted QPSK—Demodulator with IF Differential Detector

This scheme circumvents the need for local oscillators (LO), see Fig. 2.38, by using a delay line and 90° phase shifter to implement the quadrature, and two phase detectors, see Fig. 2.39. The operation is as follows (the numbers correspond to those in diagram of Fig. 2.39): (1) The received signal is converted to intermediate frequency (IF) and band-pass filtered; the bandpass filter is designed to match the transmitted pulse shape to preserve carrier phase and minimize noise power; (2) The received IF is differentially decoded using delay line and two mixers; (3) Similar to baseband differential detector already discussed [3].

2.7.5.4 $\pi/4$ QPSK Demodulator: FM Discriminator

This scheme operates as follows (the numbers correspond to those in diagram of Fig. 2.40): (1) The input signal is first filtered using a bandpass filter (BPF) that

Fig. 2.39 $\pi/4$ QPSK Demodulator IF Differential DetectorFig. 2.40 $\pi/4$ QPSK Demodulator: FM Discriminator

is matched to the transmitted signal; (2) The filtered signal is passed by a hard-limiter to minimize fluctuations in its envelope; (3) The FM discriminator extracts the instantaneous frequency; (4) The extracted signal is integrated over each period giving the phase difference between two sampling instants [3].

2.7.6 Binary Frequency-Shift Keying—BFSK

In this scheme, the frequency of a constant-amplitude carrier is switched between two values (bits 1 and 0). Then, depending on how frequency changes, there may be discontinuous phase or continuous phase between bits. The BFSK signal is given by [3],

$$s_{BFSK}(t) = \sqrt{\frac{2E_b}{T_b}} \cos(2\pi f_c + 2\pi \Delta f_c)t \quad 0 \leq t \leq T_b \quad (\text{binary } 1) \quad (2.61)$$

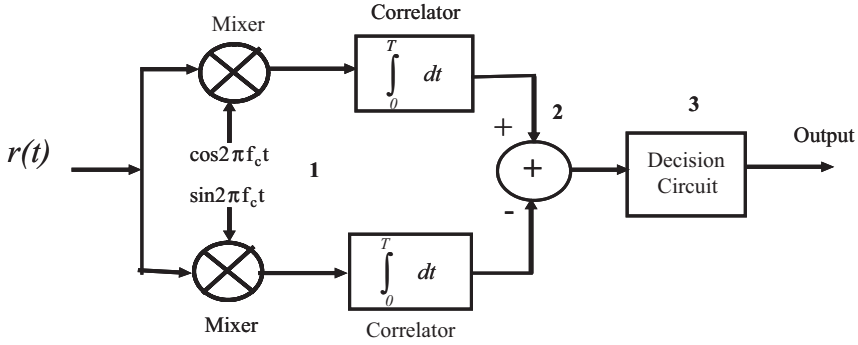


Fig. 2.41 BFSK demodulator: Coherent detector

or

$$s_{BFSK}(t) = \sqrt{\frac{2E_b}{T_b}} \cos(2\pi f_c - 2\pi \Delta f)t \quad 0 \leq t \leq T_b \quad (\text{binary } 0) \quad (2.62)$$

which is synthesized by,

$$s_{BFSK}(t) = \sqrt{\frac{2E_b}{T_b}} \cos(2\pi f_c t + 2\pi k_f \int_{-\infty}^{\infty} m(\xi) d\xi) \quad (2.63)$$

It is noticed that, even if $m(t)$ is discontinuous, due to the integration, the phase is continuous [3].

2.7.6.1 BFSK Modulator

The most common way to effect BPSK modulation is direct FM, that is, modulating the frequency of an oscillator with the message signal [3].

2.7.6.2 BFSK Demodulator: Coherent Detector

This demodulation scheme is implemented as shown in Fig. 2.41, and operates as follows (the numbers correspond to those in diagram): (1) Two correlators are applied to reference signals that are generated locally and that are *coherent*; (2) The difference of the correlator outputs is then compared in a threshold comparator; (3) The output signal is the result of the comparison, in particular, if the difference signal has a value greater than the threshold, it is classified as “1”, otherwise it is classified as a “0.” The probability of bit error is given by [3],

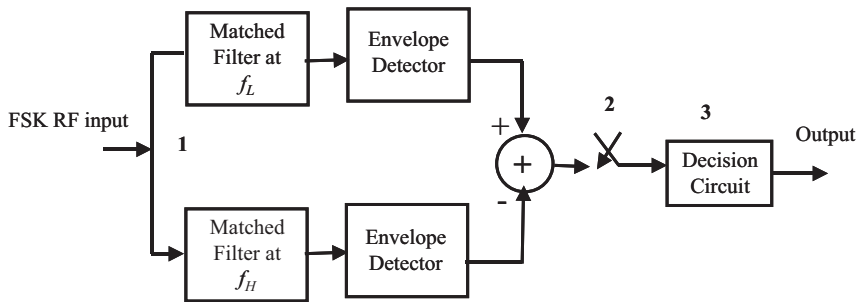


Fig. 2.42 BFSK demodulator: Noncoherent detector

$$P_{e,BPSK} = Q\left(\sqrt{\frac{E_b}{N_0}}\right) \quad (2.64)$$

2.7.6.3 BFSK Demodulator: Noncoherent Detector

To demodulate the BFSK signal, the block diagram shown in Fig. 2.42 is employed; it operates as follows (the numbers correspond to those in diagram): (1) The incoming signal is first split into two paths, namely, a lower path where it is passed through a filter that is matched to the frequency f_H , and an upper path where it is passed by a filter matched to the frequency f_L ; (2) The matched filters function as bandpass filters centered at f_H and f_L , and are passed through envelope detectors; (3) The difference of the outputs of the envelope detectors is then sampled at times $t = kT_b$; (4) Depending on the magnitude of the sampled value, the decision circuit decides the bit classification as 1 or 0. The probability of bit error rate is [3],

$$P_{e,FSK,NC} = \frac{1}{2} \exp\left(\frac{-E_b}{2N_0}\right) \quad (2.65)$$

2.7.7 Minimum Shift Keying—MSK

The MSK modulation approach entails producing a peak deviation in the frequency, equal to one-quarter the bit rate; since it is a special type of continuous phase-frequency shift keying (CPFSK), MSK is also denoted continuous FSK, with modulation index of 0.5. In general, the modulation index for this scheme is defined as: $k_{FSK} = (2\Delta F)/R_b$, where ΔF is the peak deviation; R_b is bit rate. Mobile radio systems frequently use MSK due to its spectrally efficient modulation scheme. MSK possesses: (1) Constant envelope; (2) Good BER performance; (3) Self-synchronizing capability [3].

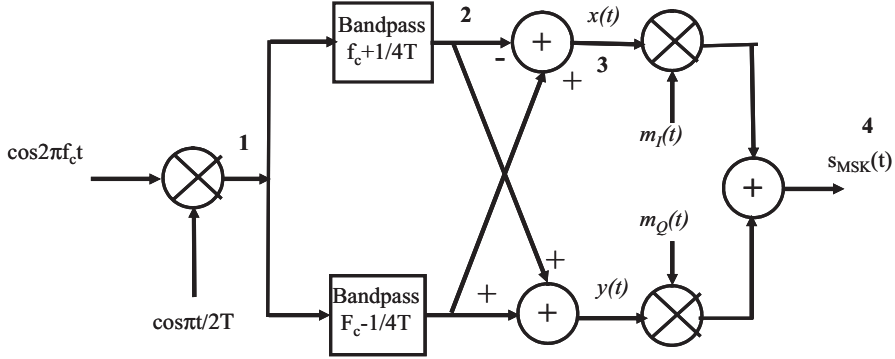


Fig. 2.43 MSK modulator

The MSK signal is given by,

$$s_{MSK}(t) = \sum_{i=0}^{N-1} m_{I_i}(t) p(t - 2iT_b) \cos 2\pi f_c t + \sum_{i=0}^{N-1} m_{Q_i}(t) p(t - 2iT_b - T_b) \sin 2\pi f_c t \quad (2.66)$$

where,

$$p(t) = \begin{cases} \cos\left(\frac{\pi t}{2T_b}\right) & 0 \leq t \leq 2T_b \\ 0 & \text{elsewhere} \end{cases} \quad (2.67)$$

where m_I and m_Q are the even and odd bits of a bipolar serial data stream with values ± 1 ; they are fed at the rate $R_b/2$ [3]. The MSK waveform may be represented by,

$$s_{MSK}(t) = \sqrt{\frac{2E_b}{T_b}} \cos(2\pi f_c t - m_{I_i}(t) m_{Q_i}(t) \frac{\pi t}{2T_b} + \phi_k) \quad (2.68)$$

MSK may be visualized as a special type of continuous phase FSK, in which ϕ_k is 0 or π depending on whether $m_I(t)$ is 1 or -1 [3].

2.7.7.1 MSK Modulator

The block diagram of the MSK modulator is shown in Fig. 2.43, and its operation is as follows (the numbers correspond to those in diagram): (1) The carrier is multiplied with $\cos(\pi/2T)$ to produce two-phase-coherent signals at $f_c + 1/4T$ and $f_c - 1/4T$; (2) The two FSK signals are separated using two bandpass filters centered at the respective frequencies; (3) And combined to form in-phase and quadrature carrier components, $x(t)$ and $y(t)$, respectively; (4) These carriers are multiplied with even and odd bit streams, $m_I(t)$ and $m_Q(t)$ to produce $s_{MSK}(t)$.

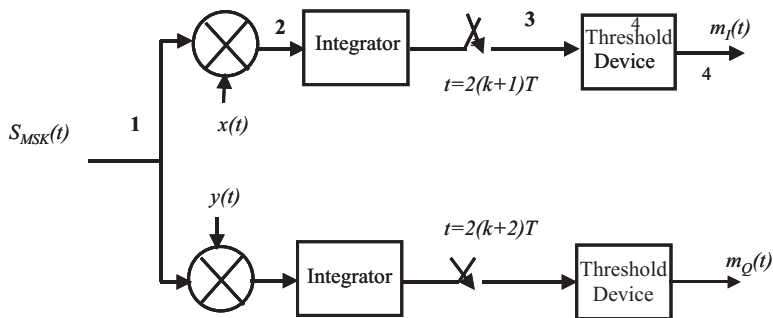


Fig. 2.44 MSK demodulator

2.7.7.2 MSK Demodulator

The block diagram of the MSK demodulator is shown in Fig. 2.44, and its operation is as follows (the numbers correspond to those in diagram): (1) First, the received incoming signal is multiplied by the respective in-phase and quadrature carriers $x(t)$ and $y(t)$; (2) The output of the multipliers are integrated over two bit periods and dumped to a decision circuit at the end of the period; (3) Based on the level of the signal, a threshold detector decides its classification as 1 or 0; (4) The output data streams correspond to $m_I(t)$ and $m_Q(t)$, which are offset to obtain the demodulated signal.

2.7.8 M-ary QAM—Quadrature Amplitude Modulation

In this scheme, the carrier amplitude is allowed to vary together with the phase. The signal is given by,

$$s_i(t) = \sqrt{\frac{2E_{\min}}{T_s}} a_i \cos(2\pi f_c t) + \sqrt{\frac{2E_{\min}}{T_s}} b_i \sin(2\pi f_c t) \quad (2.69)$$

$$0 \leq t \leq T \quad i = 1, 2, \dots, M$$

where E_{\min} is the energy of the signal with the lowest amplitude, and a_i and b_i are a pair of independent integers according to location of a signal point. The pertinent constellation for, e.g., $M = 16$, is as given in Fig. 2.45.

2.7.9 OFDM—Orthogonal Frequency Multiplexing

The OFDM approach to signal transmission provides power-efficient signaling for a large number of users in the same channel. In this scheme, multiple sub-carriers

Fig. 2.45 Constellation of M-ary QAM ($M=16$)

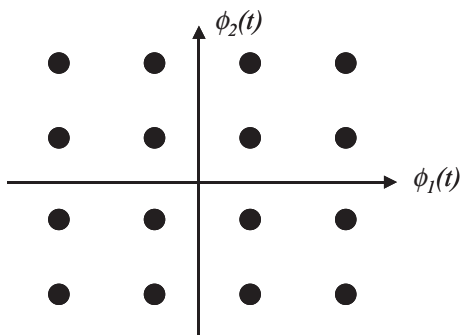
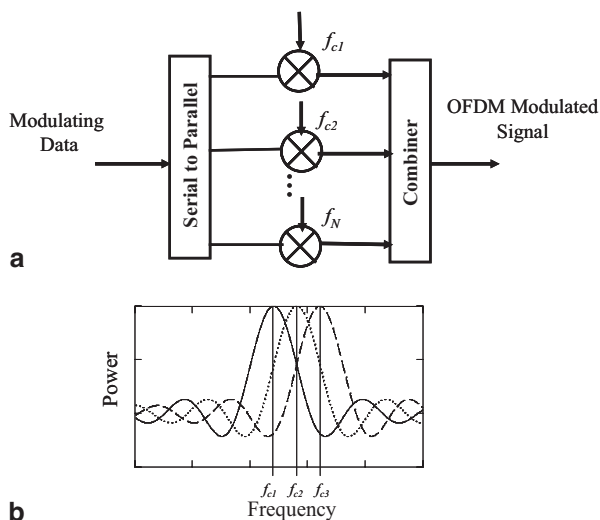


Fig. 2.46 **a** OFDM modulator block diagram. **b** Carriers modulated by rectangularly-shaped data pulses are densely spaced and orthogonal in frequency. After [1]



are employed to transmit signal bits in parallel for very high throughput. The spectra of different sub-channels can partly overlap and pulse shaping is not necessary. OFDM is usually combined with QAM or M-PSK [1] (Fig. 2.46).

2.7.10 Direct Sequence Spread Spectrum Modulation

The idea behind the direct sequence (DS) spread spectrum (SS) scheme, depicted in Fig. 2.47, is to greatly expand or spread the carrier spectrum relative to the information rate [6]. The spread spectrum signal attains an anti-jamming capability by forcing the jammer to deploy the transmitted power over a much wider bandwidth than would be necessary for a conventional system [6]. In other words, for a given jammer power, the jamming power spectral density is reduced in proportion to the ratio of the spread bandwidth B_s to the un-spread bandwidth B .

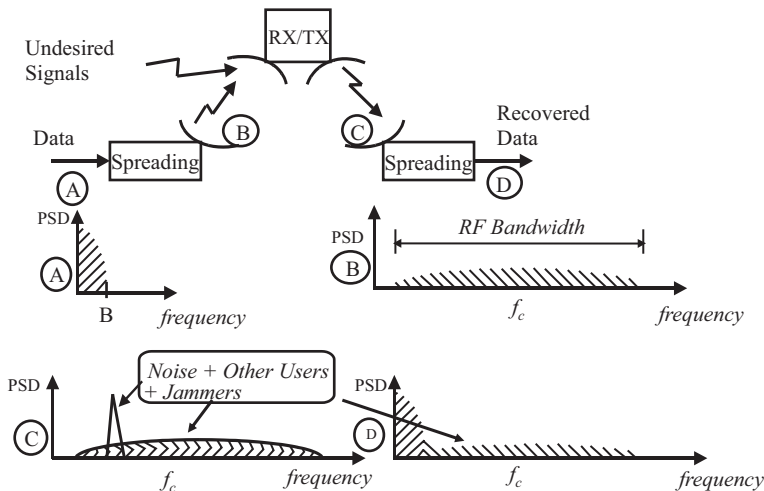


Fig. 2.47 Direct sequence spread spectrum modulation concept

2.7.10.1 Direct Sequence Spread Spectrum Modulation/Demodulation

DS/SS modulator and demodulator block diagrams are shown in Fig. 2.48. To produce an SS signal, the input data is passed through a data encoder and a data modulator, which results in the signal message $m(t)$. $m(t)$ is subsequently applied to a mixer, where it is multiplied by the product of the carrier and a pseudorandom sequence (a random-like signal of ± 1 $p(t)$) to produce [6],

$$V_{ss}(t) = \sqrt{\frac{2E_s}{T_s}} m(t) p(t) \cos(2\pi f_c t + \theta) \quad (2.70)$$

where,

$$m(t) = \sum_{m=-\infty}^{\infty} a_m p_m(t - mT_b) \quad (2.71)$$

and

$$p(t) = \sum_{n=-\infty}^{\infty} c_n p'(t - nT_c) \quad (2.72)$$

The DS/SS system is employed in Code Division Multiple Access (CDMA), where each user has pseudo-noise (PN) sequence, and multiple users share the same BW; the signals of one user appearing as noise to others. A feedback shift register with

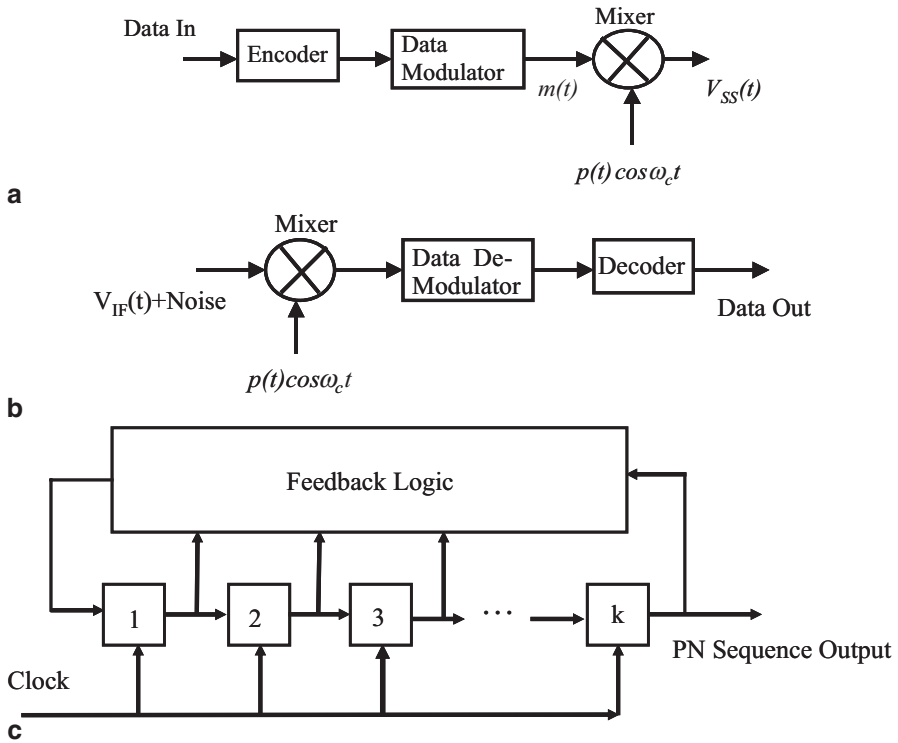


Fig. 2.48 Direct sequence spread spectrum: **a** Modulator. **b** Demodulator. **c** PN sequence generator diagram

k stages is employed for generating the PN sequence, (2.72), Fig. 2.48c. For a shift register of k stages, the PN sequence length is $N = 2^k - 1$ [6]. The measure of interference rejection of a DS/SS system is given by the so-called *processing gain*, defined by,

$$PG_{DS} = \frac{T_b}{T_c} = \frac{R_c}{R_b} \quad (2.73)$$

2.7.11 Frequency Hopping Spread Spectrum Modulation/Demodulation

The frequency hopping (FH) spread spectrum scheme, Fig. 2.49, involves the periodic change of the transmission frequency [6]. In this scheme a sequence of modulated data bursts with time-varying, pseudo-random carrier frequencies, is transmitted. In FH the processing gain is given by,

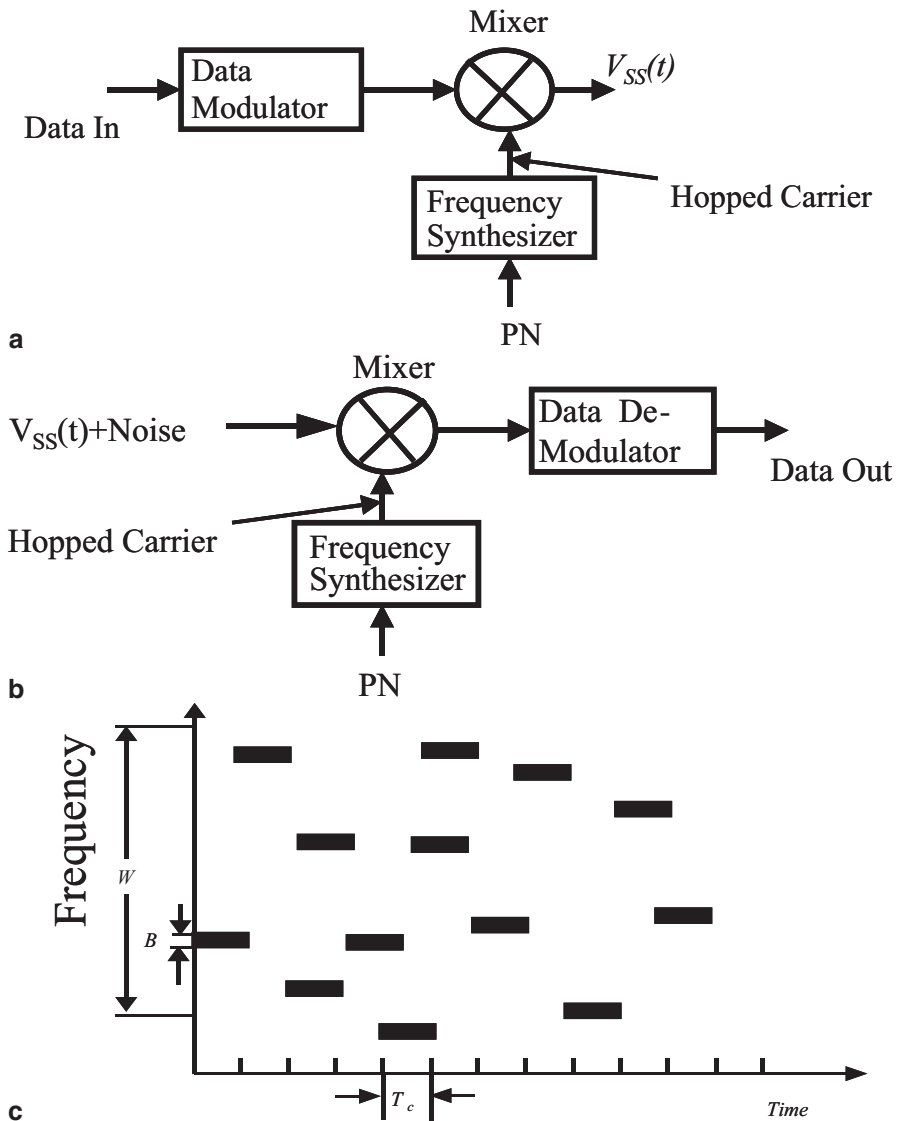


Fig. 2.49 Frequency hopping spread spectrum: **a** Modulator. **b** Demodulator. **c** Frequency hopping versus time. T_c is the duration of time in a given frequency band

$$PG_{FHS} = \frac{W}{B} \quad (2.74)$$

where, W is the frequency range through hopping can occur, and B is the bandwidth of the band being hopped [6].

2.8 Summary

In this chapter, we have addressed a number of topics surrounding modulation and demodulation, with emphasis in familiarizing the reader with their *system-level* block diagrams. We began by introducing system-level block diagrams of AM and FM/PM modulators and demodulators, and explaining their respective principles of operation. In particular, under the topic of AM Modulator/Demodulator, we introduced the full carrier modulator, the single sideband suppressed carrier modulator, the double sideband suppressed carrier modulator, the envelope detector, and the synchronous detector. Under the topic of FM and PM Modulator/Demodulator, we introduced the VCO as FM modulator, the indirect FM modulator, the PM modulator, the balanced discriminator FM demodulator, the quadrature FM detector, the PLL-based FM detector, the zero-crossing FM detector, and the PM demodulator. Then, under the topic of digital modulation, we introduced the concepts of Nyquist Limit, data rate, Shannon Limit, information capacity, and bandwidth efficiency, as well as specific modulation schemes, such as, binary modulation, amplitude-shift keying (BASK), frequency-shift keying (BFSK), and phase-shift keying (BPSK), differential binary phase-shift keying (DBPSK), quadrature phase-shift keying (QPSK), $\pi/4$ shifted QPSK, minimum shift keying (MSK), M-ary quadrature amplitude modulation (QAM), orthogonal frequency division multiplexing (OFDM), direct sequence spread spectrum (DS/SS), and frequency hopping spread spectrum (FH/SS). We also introduced the geometric representation of digital modulation schemes and the complex envelope form of a modulation signal.

References

1. J. Dąbrowski, Course “Introduction to RF Electronics,” Lecture Notes; Division of Electronic Devices, Department of Electrical Engineering (ISY), Linköping University, 2006.
2. Mischa Schwartz, *Information Transmission, Modulation, and Noise*, McGraw-Hill, 1970.
3. T. S. Rappaport, *Wireless Communications: Principles and Practice*, Second Ed., Prentice-Hall, Inc. 2002.
4. H. J. De Los Santos, Lecture Notes, “Communications Circuits,” Course EE115D, Department of Electrical Engineering, University of California, Los Angeles (UCLA), Fall Quarter, 1990.
5. Q. Gu, *RF System Design of Transceivers for Wireless Communications*, Springer, 2005.
6. R. C. Dixon, *Spread Spectrum Systems with Commercial Applications*, Third Edition, John Wiley & Sons, Inc., New York, 1994.
7. Available: [Online]: <http://www.clee.freehomepage.com/teaching.html/>

Radio Systems Engineering

A Tutorial Approach

De Los Santos, H.J.; Sturm, C.; Ponte, J.

2015, XVI, 253 p. 218 illus., 28 illus. in color., Hardcover

ISBN: 978-3-319-07325-5